

New Jersey Institute of Technology Digital Commons @ NJIT

Theses

Theses and Dissertations

Spring 2016

An electromechanical system for characterization of piezoelectric materials

Ahmet Sait Asan

New Jersey Institute of Technology

Follow this and additional works at: <https://digitalcommons.njit.edu/theses>



Part of the [Biomedical Engineering and Bioengineering Commons](#)

Recommended Citation

Asan, Ahmet Sait, "An electromechanical system for characterization of piezoelectric materials" (2016). *Theses*. 267.
<https://digitalcommons.njit.edu/theses/267>

This Thesis is brought to you for free and open access by the Theses and Dissertations at Digital Commons @ NJIT. It has been accepted for inclusion in Theses by an authorized administrator of Digital Commons @ NJIT. For more information, please contact digitalcommons@njit.edu.

Copyright Warning & Restrictions

The copyright law of the United States (Title 17, United States Code) governs the making of photocopies or other reproductions of copyrighted material.

Under certain conditions specified in the law, libraries and archives are authorized to furnish a photocopy or other reproduction. One of these specified conditions is that the photocopy or reproduction is not to be “used for any purpose other than private study, scholarship, or research.” If a user makes a request for, or later uses, a photocopy or reproduction for purposes in excess of “fair use” that user may be liable for copyright infringement,

This institution reserves the right to refuse to accept a copying order if, in its judgment, fulfillment of the order would involve violation of copyright law.

Please Note: The author retains the copyright while the New Jersey Institute of Technology reserves the right to distribute this thesis or dissertation

Printing note: If you do not wish to print this page, then select “Pages from: first page # to: last page #” on the print dialog screen

The Van Houten library has removed some of the personal information and all signatures from the approval page and biographical sketches of theses and dissertations in order to protect the identity of NJIT graduates and faculty.

ABSTRACT

AN ELECTROMECHANICAL SYSTEM FOR CHARACTERIZATION OF PIEZOELECTRIC MATERIALS

**by
Ahmet Sait Asan**

Piezoelectric materials have been used in medical applications for a long time due to their unique characteristics, which is to respond to mechanical stimulation by producing an electrical current and vice versa. They perform a pivotal role in medical applications both for diagnostic and therapeutic purposes. In this regard, characterizing the piezoelectric properties of these materials is crucial for their usage. In this particular study, an electromechanical system for measurement of piezoelectric output signals is designed and tested. The project is motivated by the question: can the piezoelectric properties be characterized by applying different mechanical stimulation waveforms and frequencies. Two well-known piezoelectric materials, Polyvinylidene Fluoride (PVDF) and Lead Zirconate Titanate (PZT), are used as samples in this project to demonstrate the device operation. In addition, a non-piezoelectric material is included as a control group.

**AN ELECTROMECHANICAL SYSTEM FOR CHARACTERIZATION OF
PIEZOELECTRIC MATERIALS**

by
Ahmet Sait Asan

**A Thesis
Submitted to the Faculty of
New Jersey Institute of Technology
in Partial Fulfillment of the Requirements for the Degree of
Master of Science in Biomedical Engineering**

**Department of Biomedical Engineering
May 2016**

APPROVAL PAGE

**AN ELECTROMECHANICAL SYSTEM FOR CHARACTERIZATION OF
PIEZOELECTRIC POTENTIALS**

Ahmet Sait Asan

Dr. Mesut Sahin, Thesis Advisor Date
Professor of Biomedical Engineering, NJIT

Dr. Treena L Arinzeh, Committee Member Date
Professor of Biomedical Engineering, NJIT

Dr. Max Roman, Committee Member Date
Assistant Research Professor of Biomedical Engineering, NJIT

BIOGRAPHICAL SKETCH

Author: Ahmet Sait Asan

Degree: Master of Science

Date: May 2016

Undergraduate and Graduate Education:

- Master of Science in Biomedical Engineering,
New Jersey Institute of Technology, Newark, NJ, 2016
- Bachelor of Science in Mechatronics Engineering,
Kocaeli University, Kocaeli, Turkey, 2012

Major: Biomedical Engineering

Minds should be enlightened with science, and hearts need to be illumined with religion. The truth comes forth by the marriage of the two.

Vicdanın ziyası, ulûm-u diniyedir. Aklın nuru, fûnun-u medeniyedir. İkinin imtizacıyla hakikat tecellî eder.

ACKNOWLEDGMENT

First and foremost, I would like to express my sincere gratitude to my advisor Dr. Mesut Sahin. I could not finish my thesis without his guidance, deep knowledge, and support. I would also like to thank my committee members, Dr. Treena L. Arinze and Dr. Max Roman for their time, and valuable comments.

I also owe a special debt to Neural Interface lab members, Dr. Ali Ersen, Sinan Gok, and Ferhat Erdogan for their help and support. Finally, I would like to thank my family for their support and encouragement.

TABLE OF CONTENTS

Chapter	Page
1 INTRODUCTION.....	1
1.1 Objective	1
1.2 Organization.....	2
2 BACKGROUND.....	3
2.1 Dielectric Materials.....	3
2.1.1 Polar Effects.....	4
2.1.2 History of Piezoelectricity.....	4
2.2 Piezoelectricity.....	5
2.2.1 Piezoelectric Effect.....	6
2.2.1.1 Indirect Piezoelectric Effect.....	6
2.2.1.2 Direct Piezoelectric Effect.....	7
2.3 Materials Properties.....	9
2.4 Dynamics Behavior of Piezoelectric Materials.....	11
2.5 Piezoelectric Materials.....	12
2.5.1 Quartz.....	13
2.5.2 Piezoceramic.....	13
2.5.3 Piezopolymer.....	13
2.5.4 Piezocomposite.....	14
2.7 Polyvinylidene Fluoride (PVDF).....	14
2.8 PVDF Scaffold.....	15
2.9 Application of Piezoelectricity.....	16

TABLE OF CONTENTS
(Continued)

Chapter	Page
2.10 Piezoelectric Actuator.....	17
2.11 Longitudinal Actuator.....	17
3 RESEARCH DESIGN AND METHODOLOGY.....	19
3.1 Overall System Description.....	19
3.2 DAQ Board... ..	20
3.3 BK Precision Signal Generator.....	21
3.4 Amplifier.....	23
3.5 Force Sensor	23
3.6 Charge amplifier.....	24
3.7 Stack Piezoelectric Actuator.....	24 37
3.8 Faraday Cage	25 42
3.9 Experimental Procedure.....	26
4 RESULTS and DISCUSSION.....	32
4.1 Stack Piezoelectric Actuator Response to Varying Voltages.....	32
4.2 Stack Piezoelectric Actuator’s Response to Various Waveforms.....	35
4.3 Sinusoidal Excitation of the Stack Actuator	36
4.4 Metallic PVDF Measurement.....	37
4.5 PZT Measurement.....	41
4.6 Non-Piezoelectric Material Measurement.....	45
4.7 Piezoelectric vs. Non-piezoelectric.....	46
4.8 Design Comparison.....	46

TABLE OF CONTENTS
(Continued)

Chapter	Page
5 CONCLUSION AND FUTURE WORK.....	48
5.1 Conclusion.....	48
5.2 Future Work.....	49
APPENDIX MATLAB SOURCE CODES	51
REFERENCES.....	56

LIST OF FIGURES

Figure	Page
2.1 The bound charges are touching the capacitor plates while the free charges usually float around in the material, but for this case, they are aligned with the bound charges	4
2.2 Classification of dielectric materials	6
2.3 Indirect piezoelectric effect: (a) Poled piezoelectric material. (b) When a DC field is applied with the same polarity as the poling field, the materials develops tensile. (c) When a DC field is applied in the reverse direction, the material develops compressive strain.....	8
2.4 Direct piezoelectric effect: (a) Poled piezoelectric materials. (b) When tensile stress is applied to the material, the material develops voltage across its face with the same polarity as the poling voltage. (c) When a compressive stress is applied to the material, the material develops voltage with polarity opposite to that of the poling voltage.	9
2.5 Effect of AC field on a piezoelectric: (a) Poled piezoelectric material; (b) AC field is applied to the material. The material gets extended and contracted alternately; that is, the material vibrates producing an acoustic field in the vicinity.....	10
2.6 Equivalent electrical circuit representation of vibrating piezoelectric element.....	12
2.7 A typical electrospinning setup. A polymer solution (blue) is dispensed from a syringe pump (orange). A high voltage DC power supply (green) grounds a rapidly rotating wheel collector (grey) onto which aligned nanofibers are collected. The polymer jet between the syringe and collector consists of a steady streaming segment and a rapidly oscillating whipping segment.....	15
2.8 (a) Needle and collector distance vs. fiber diameter. (b) Flow speed vs. fiber diameter. (c) Viscosity vs. fiber diameter. (d) Applied electrical field vs. fiber diameter.....	16
2.9 Possible configuration of electric field lines between the needle system and the collector.....	17

LIST OF FIGURES
(Continued)

Figure	Page
2.10 Category of electrospinning setups based on rotating device. These configuration include (a) solid cylindrical, (b) wire wound on an insulated cylinder, (C) wired drum, (d) disc collector, (e) sharp pin inside the rotating collector, (f) knife-edge electrodes, and (g) knife-edge electrode and needle system.....	17
2.11 Longitudinal displacement (top) and polarization of the individual layers (bottom) of a stack actuator.....	22
3.1 Block diagram of data acquisition of applying stress to the piezoelectric material into the computer via the NI DAQ Board.....	23
3.2 PCI 6259 DAQ Board, maximum sampling frequency is 1.25 MHz	25
3.3 BK Precision Signal Generator.....	26
3.4 EPA-008-1 Linear Amplifier	27
3.5 Charge amplifier circuit.....	28
3.6 FS03 Force sensor	28
3.7 Piezoelectric stack actuator	29
3.8 Faraday Cage.....	30
3.9 Piezoelectric stack actuator	30
3.10 Micromanipulator	31
3.11 Electrodes and force sensor.....	32
3.12 Charge amplifier.....	33
3.13 General view of the design.....	34
3.14 General view of the design with faraday cage.....	35

LIST OF FIGURES
(Continued)

Figure	Page
4.1 Output voltage of the force sensor at increasing voltages applied to the piezoelectric actuator.....	36
4.2 Correlation of the generated force by actuator and actuator's input voltage.....	37
4.3 Force sensor output to different waveforms.....	39
4.4 Measured peak force at different frequencies of waveform.....	40
4.5 The PVDF response at different force amplitudes varied (between 0.13 and 0.81).....	41
4.6 The PVDF response at different force amplitudes varied (between 0.98 and 1.3)	42
4.7 A linear line fit to the PVDF output data.....	43
4.8 The PZT output voltage vs. the Force.....	45
4.9 Force sensor output.....	47
4.10 PZT output.....	48
4.11 Relationship with force non-piezoelectric material output.....	49
4.12 Comparison between PVDF and non-piezoelectric materials output.....	50

CHAPTER 1

INTRODUCTION

1.1 Objectives

The objective of this thesis is to characterize piezoelectric materials' behavior. Piezoelectric materials have the ability to convert mechanical energy type to electrical and vice versa, and that makes them particularly important for biomedical applications. Tissue recovery, piezosurgery, and pressure sensing are some of the areas where piezoelectric materials find applications in medicine.

The thesis implements a novel design to characterize piezoelectric materials performance. A stack piezoelectric actuator was employed to apply mechanical stress to the materials under testing, and piezoelectric materials' output and the applied force were collected simultaneously to estimate the d_{33} value. In order to test the system the Polyvinylidene Fluoride (PVDF), Lead Zirconate Titanate (PZT), and a non-piezoelectric material samples were used.

This design is able to generate a force in various waveforms and at different frequencies applied to the material. Also for further signal processing, the collected force and piezoelectric charge output signals are acquired into a computer. Being able to apply mechanical perturbations in different waveforms is the advantage of this setup over other commercially available designs. Another key point for this design is that with a small modification the system can begin testing piezoelectric materials in wet conditions, which is a necessary step for better understanding how PVDF scaffold behave *in vivo*.

1.2 Organization

This thesis is divided into five chapters. This chapter presents the objectives and the significance of this work. Chapter 2 reviews the theoretical background for this study. Chapter 3 provides information about the experimental setup and the main components of the design. Chapter 4 shows the results of preliminary testing using selected materials. Finally, Chapter 5 presents the conclusion of the work along with future outlook.

CHAPTER 2

INTRODUCTION

2.1 Dielectric Materials

Dielectric materials have a poor performance to convey electricity. However, when they are exposed to external electrical fields, these materials can store and carry charges for short ranges. Solid materials include positive and negative charges, but under the influence of an electrical field, these charges separate to the positive and negative group (Stroyan 2004). This phenomenon is called polarization. One of the crucial types of dielectric materials is piezoelectric materials which are utilizing this separation in order to convert one energy type to another one.

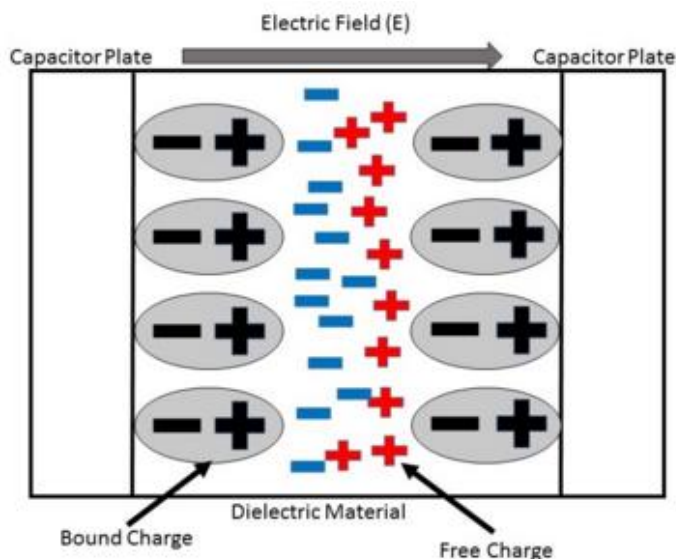


Figure 2.1 The bound charges are touching the capacitor plates while the free charges usually float around in the material, but for this case, they are aligned with the bound charges.

Source: The Dynamic Chemistry Hypertext.

2.1.1 Polar Effects

Crystal structure of the materials defines their characteristics. Piezoelectricity, pyroelectricity, and ferroelectricity are some of the important features that certain materials have (Stroyan 2004). Due to these characteristics, piezoelectric, pyroelectric, and ferroelectric materials become polarized when they are exposed to mechanical stress. In other words, these materials can convert mechanical energy to electrical energy or vice versa. Pyroelectric materials convert the heat energy to the electrical energy because pyroelectric materials' crystal structure changes when they are under the effect of temperature change. The opposite case is also valid for their crystal structure. When a ferroelectric material is subjected to an electrical field, its crystal structure is polarized until the electrical effect is removed.

2.1.2 History of Piezoelectric Materials

Piezoelectricity was first realized in the early part of 18th century. As tourmaline crystals were thrown in hot ashes, it was noticed that these crystals attracted and repelled the ashes. However, the researchers did not know this was piezoelectricity. German physicist Aepinus explained the reason of this interesting movement of the tourmaline crystals. According to the German scientist, the reason for this behavior was of the electrical origin. Scottish physicist D. Brewster called this behavior pyroelectricity in 1824 (Cady 1946).

In 1880, Piezoelectricity was discovered by Pierre and Jacques Curie. At the beginning of their scientific careers, Curie brothers realized that under compression, certain types of crystals produced charges on their surfaces. Eventually, the two brothers developed the basics of piezoelectric behavior and documented responses of the materials

like Rochelle salt, quartz, and topaz. Walter Guyton Cady provided in his book, *Piezoelectricity*, the core understanding of piezoelectricity in 1946.

2.2 Piezoelectricity

Because of the inner polarization of the materials, when dielectric materials are subjected to an external electric field, the dimensions of the materials change. The reason is that under the electrical influence, negative charges move in the direction of the electrical field, and positive charges move in the opposite way of the electrical field. These specific movements cause materials to change their shape (Vijaya 2013).

Crystals are classified into 32 classes, 21 of them have the non-center-of-symmetry, and the rest of them have the center-of-symmetry.

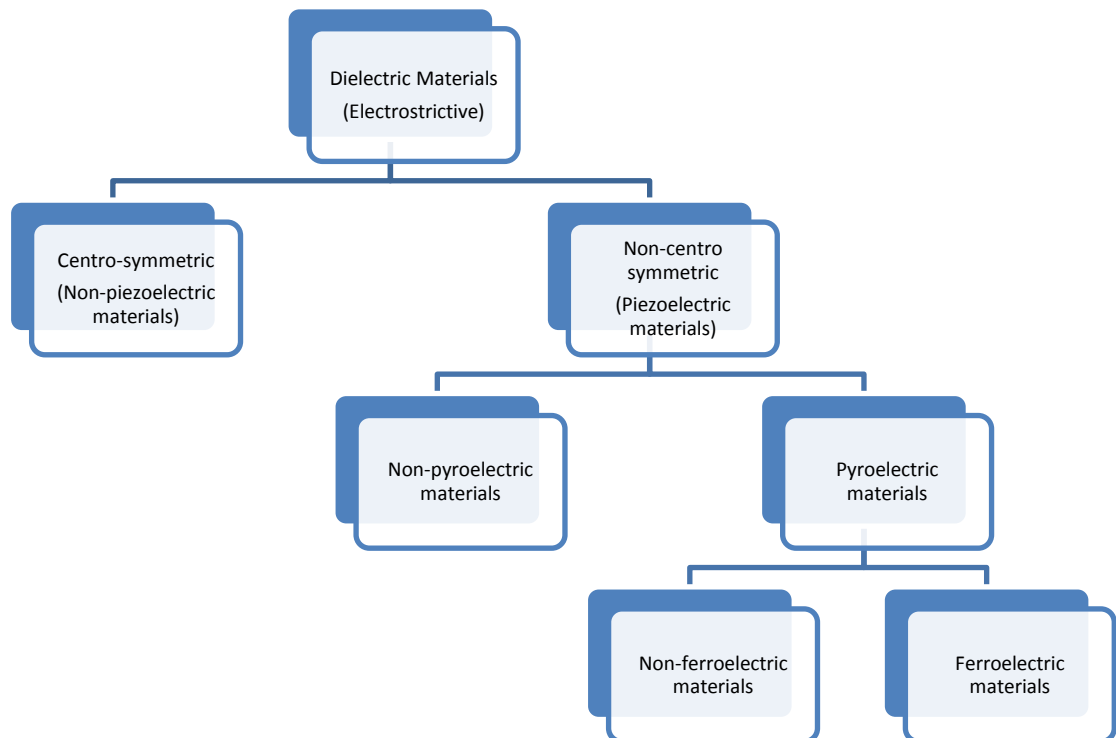


Figure 2.1 Classification of dielectric materials.

Source: Vijaya, M. S. (2013). *Piezoelectric materials and devices*. CRC Press: Boca Raton, FL.

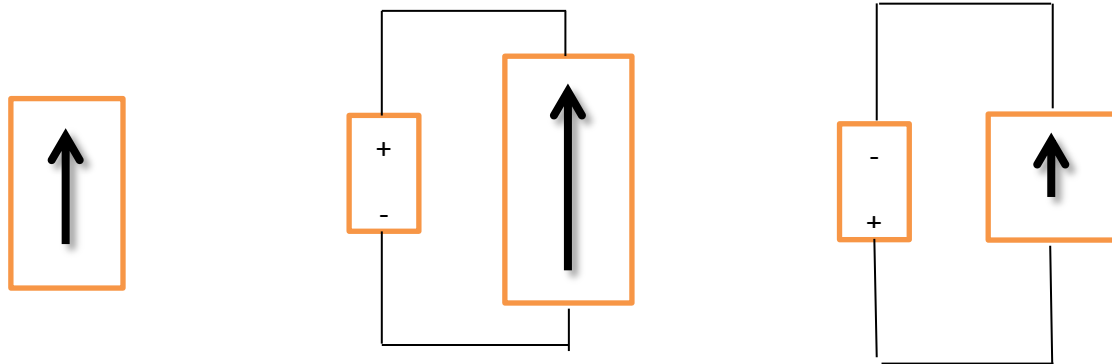
When the centro-symmetric materials undergo an external electrical field, due to the symmetrical structure, positive and negative charges' contractions and extensions will eliminate each other, and ideally there will be no dimensional change. However, due to the fact that chemical bonds do not perfectly match, there is still a small amount of deformation. On the other hand, if a material has the non-symmetrical structure, under the influence of the electrical field, opposite charges will move in different directions, and this will cause deformation of the material (Vijaya 2013). Piezoelectric materials have non-symmetric crystal structure. These materials are also called smart materials (Harrison and Ounaies 2001).

2.2.1 Piezoelectric Effect

Dielectric materials are divided into two categories, centro-symmetric and non-centro-symmetric. Piezoelectric materials are under the class of the non-centro-symmetric category. The piezoelectric effect is also divided into two groups: direct effect, and indirect effect.

2.2.1.1 Indirect Effect. When an electric field is applied to a non-centro-symmetric material, its positive and negative charges move asymmetrically. Asymmetrical movement causes deformation of the material. Depending on the polarity of the applied electrical field, the deformation can be either in the form of expansion or compression (Vijaya 2013).

Some of the important applications of the indirect piezoelectric effect are the sonar, piezoelectric speakers, and electromechanical transducers, which convert electricity into mechanical movements.



(a) Poled piezoelectric material.

(b) DC voltage applied to the material. Tensile strain generated.

(c) DC voltage applied with reverse polarity. Compressive strain generated.

Figure 2.2 Indirect piezoelectric effect: (a) Poled piezoelectric material. (b) When a DC field is applied with the same polarity as the poling field, the materials develop tensile strain. (c) When a DC field is applied in the reverse direction, the material develops compressive strain.

Source: Vijaya, M. S. (2013).

2.2.1.2 Direct Effect. When a mechanical tension is applied to the piezoelectric materials, due to the non-symmetrical structure of the piezoelectric materials, a potential difference occurs on the two sides of the material's surface, and a voltage output can be measured. The more stress is applied to the material, the larger voltage can be measured (Vijaya 2013).

Piezoelectric device are dynamic systems, hence, if a stable mechanical stress is applied to the piezoelectric material, the output of the material will not be stable; on the contrary, it will decay due to the internal finite impedance of the piezoelectric material. Therefore, a charge amplifier can be employed to collect the charges before they dissipate. Using the direct piezoelectricity is vital for many sensor applications. Pressure, force, and acceleration sensors are some examples of the piezoelectric sensor systems.

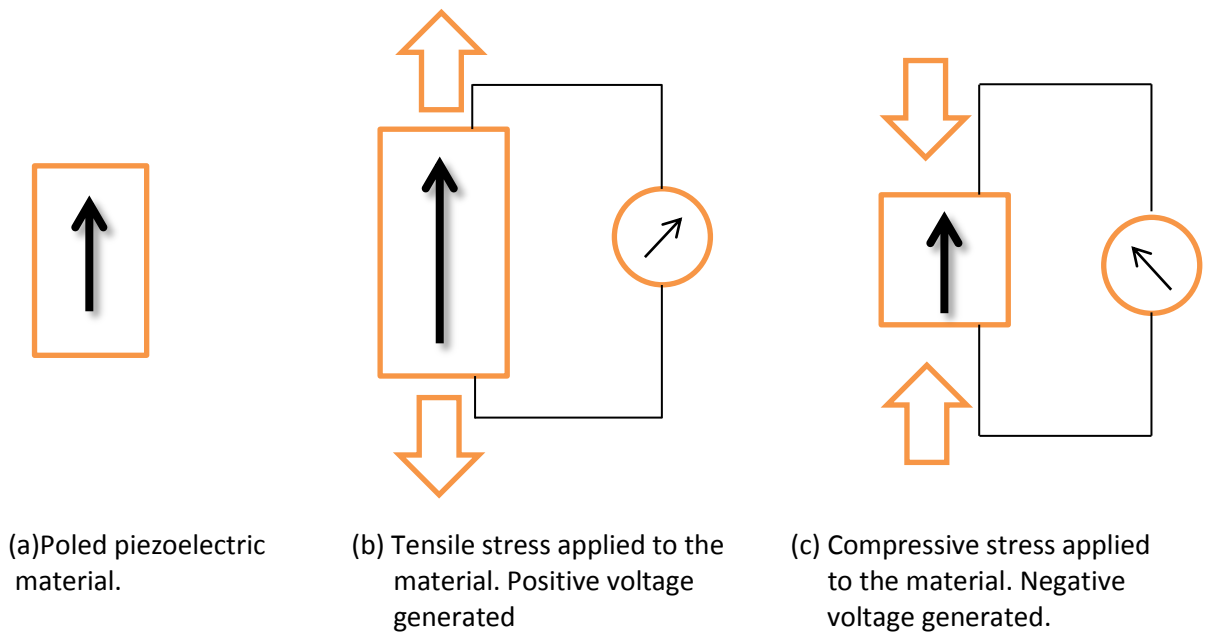


Figure 2.3 Direct piezoelectric effect: (a) Poled piezoelectric materials. (b) When tensile stress is applied to the material, the material develops a voltage across its face with the same polarity as the poling voltage. (c) When a compressive stress is applied to the material, the material develops voltage with polarity opposite to that of the poling voltage. Source: Vijaya, M. S. (2013).

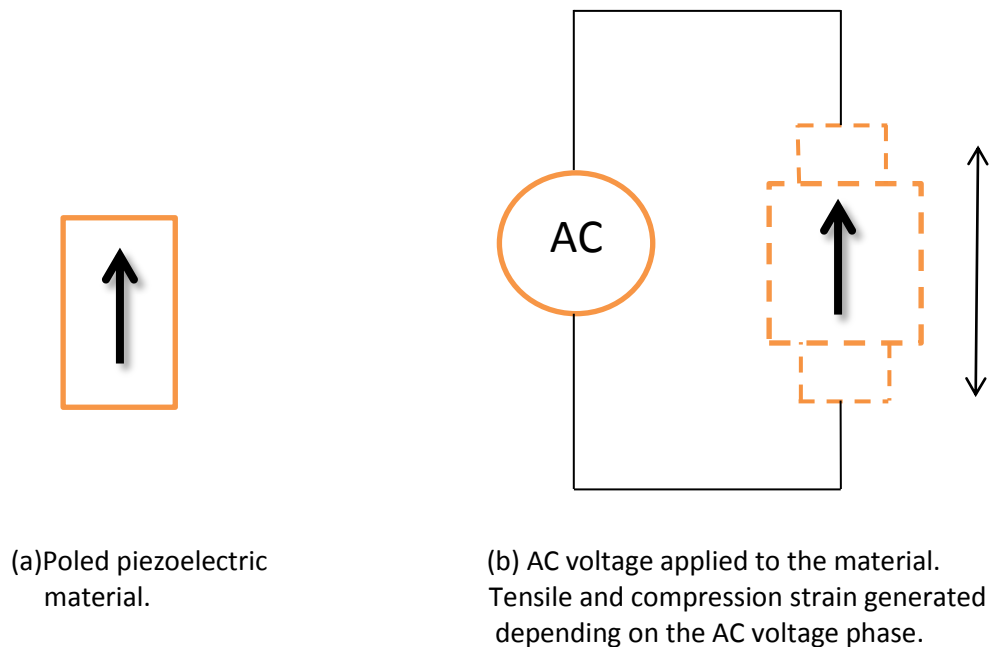


Figure 2.4 Effect of AC field on a piezoelectric: (a) Poled piezoelectric material; (b) AC field is applied to the material. The material gets extended and contracted alternately; that is, the material vibrates producing an acoustic field in the vicinity. Source: Vijaya, M. S. (2013).

The equations below are the governing equations of piezoelectric materials. They describe the two piezoelectric effects with respect to electrical and elastic properties (Haertling 1999).

$$\text{Direct Effect: } \underline{D} = d\underline{T} + \varepsilon\underline{E} \quad (2.1)$$

$$\text{Indirect Effect: } \underline{\chi} = s\underline{T} + d\underline{E} \quad (2.2)$$

D is equal to the surface charge divided by area, d is the piezoelectric coefficient, T is stress, ε is the permittivity of the material, E is the electrical field, χ is the strain, and s is the compliance or elasticity coefficient, all given as three dimensional tensors.

2.3 Material Properties

As mentioned in the section 2.2.1, there are two types of piezoelectric behaviors. The direct effect is when the input is a mechanical energy such as stress, the output will be in the electrical form, and for the indirect effect, it is vice versa as mentioned in the previous sections. To have a better understanding about the piezoelectric materials, it should be known what kinds of parameters have an impact on the piezoelectric materials. In this section, piezoelectric material properties are discussed.

Under the mechanical stress, the piezoelectric material generates electricity. This electricity depends on the piezoelectric coefficient e whose unit is N/V m (Vijaya 2013). The coupling between elastic and electrical effects depends on the magnitude of the stress constant. Strain constant d is the other critical coefficient which relates to the external electrical field. It is also called transmitting constant with the unit of m/V (Vijaya 2013).

Generated electrical field per unit of the mechanical stress is denoted by the receiving constant g , with the unit of V m/N (Vijaya 2013). Permittivity ϵ is the dielectric parameter of the piezoelectric material, and it is related to the vectors of the coefficients d and ϵ both (Vijaya 2013). Permittivity defines piezoelectric materials' electrical impedance. The relationship between the d and e coefficients is defined as (Vijaya 2013).

$$\underline{d} = \epsilon \underline{e} \quad (2.3)$$

Coupling coefficient k is another parameter to understand the efficiency of piezoelectric materials as a transducer (Vijaya 2013). It shows the material's ability to convert the energy from one type to another, which is in our case from mechanical to electrical and vice versa. While converting the energy, there can be some energy loss and eventually this causes sensitivity and bandwidth loss (Devaraju 2013). The equation below shows the relationship between them.

$$(k)^2 = \frac{(\text{piezoelectric energy density stored in the material})^2}{\text{electrical energy density} * \text{mecaanical energy density}} \quad (2.4)$$

Piezoelectric constant also reflects the same quantity.

2.4 Dynamic Behavior of a Piezoelectric Material

To understand the dynamic behavior of the piezoelectric materials, the electrical or mechanical representation of the system can be used. In this thesis, the electrical representation is employed (figure 2.6).

Figure 2.6, the alternating voltage represents applied vibrating force, and the piezoelectric material is shown as a capacitor C_0 .

$$C_0 = \frac{\varepsilon A}{d} \quad (2.5)$$

Where ε is permittivity of the material, A is the area, and d is the thickness of the material. The mass of the piezoelectric material is represented by L , and C symbolizes the compliance constant. Moreover, due to the friction and other reasons, there is energy loss in the system. R represents all the loss in the system.

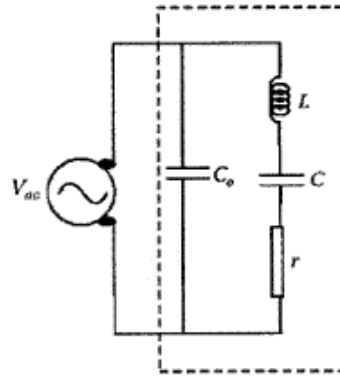


Figure 2.5 Equivalent electrical circuit representation of vibrating piezoelectric element.

Source: (Vijaya,2013).

The impedance of the system is a function of the frequency. The peak values of the impedance define a resonance. If the impedance has its minimum value, this point is

called resonance frequency; and when it has a maximum value, it is called anti-resonance frequency. A piezoelectric material reaches its maximum output voltage amplitude when it is in the resonance frequency. Assuming that the energy loss is zero, resonance frequency (f_r) becomes

$$f_r = f_s = \frac{1}{2\pi} \sqrt{\frac{1}{LC}} \quad (2.6)$$

Under the same circumstance, zero loss, anti-resonance (f_a) becomes

$$f_a = f_p = \frac{1}{2\pi} \sqrt{\frac{C+C_0}{LC C_0}} \quad (2.7)$$

Electromechanical coupling coefficient can be calculated by the help of f_r and f_a (San Emerito 1997, Vijaya 2013).

2.5 Piezoelectric Materials

Piezoelectric materials can be used in a diverse list of areas such as fabrication of micro-electrical-mechanical system (MEMS), detection of mechanical vibrations or displacements, and various biomedical areas. Piezoelectric materials will be classified in this section.

2.5.1 Quartz

Quartz is one of the most prevalent minerals in nature. It has been used as a crystal oscillator and quartz clock. Because quartz has a piezoelectric structure, it can be utilized in frequency control applications (Vijaya 2013). Robust mechanical properties, high stiffness constant, high Q factor, good reliability, and long life make the quartz ideal material to be used for resonance applications over other materials (Vijaya 2013).

2.5.2 Piezoceramics

Piezoelectric ceramic materials (PCMs) have ferroelectric connections. Solid materials such as lead zirconate titanate (PZT) are used to produce modern PCM (Sharapov 2014). PZT has some vital properties such as its electromechanical coupling coefficient in thickness mode, high relative dielectric constant, low mechanical loss, and low dielectric loss (Devaraju 2013). Due to these superior properties, it is used in many transducers and actuator applications. However, it has some drawbacks, such as fragility, low reproducibility, and fabrication difficulties.

2.5.3 Piezopolymers

There is a significant difference between the structure of the polymers and inorganics, which are crystals and ceramics. Notably, piezoelectric strain constant of the polymers is lower than ceramics. On the other hand, the piezoelectric constant is much higher than that of the ceramics. Polymers are light and tough; and that is why they find a wide range of applications as sensors and actuators. Furthermore, they are flexible, and they can easily be formed into desired shapes. Some of the other features of the polymers are high strength, high impact resistance, low electrical constant, low elastic stiffness, and low

density (Harrison 2007). Polyvinylidene fluoride (PVDF) is one of the most well-known and widely used polymers. The discovery of a large residual polarization in oriented films of PVDF has first mentioned in the Kawai's research in 1969, and it has become the cornerstone for the usage of polymers (Brown 2000).

2.5.4 Piezocomposite

Piezocomposite materials are derived from a combination of the polymers and ceramics, and this makes them special for electromechanical transducer applications (Guinovart-Díaz, Bravo-Castillero et al. 2001). Due to the high piezoelectricity and pyroelectric properties they show, they are receiving more attention in recent years. These materials provide higher operating frequencies, thereby, they improve the resolution in medical applications (Guinovart-Díaz, Bravo-Castillero et al. 2001). Finally, these materials have promising results for high-pressure sensors, hydrophones, and shock accelerometers (Zhang 2008).

2.7 Polyvinylidene Fluoride (PVDF)

Some synthetic and biomedical polymers such as wood and muscle tendons have natural piezoelectricity. Using these materials was not common, but, after Kawai's discovery, polymers had a prevalent usage (Stroyan 2004). After imposing a DC electric field and a high temperature to these polymers, it has been found that it is possible to detect piezoelectric voltages from these polymers. These materials became very popular in a short period because of their flexibility and mechanical properties.

PVDF is one of the most promising polymers in the field. The reason is that it has a fast and a large electromechanical response, high mechanical and chemical stability,

low acoustic impedance, and flexibility (Eberle, Schmidt et al. 1996, Bae and Chang 2015). Hence, it has been used in various applications such as pressure sensors, vibration measurements, ultrasonic imaging in medical instruments, and speakers (Shirinov and Schomburg 2008, Sharma, Naik et al. 2015). PVDF-based materials can also be formed in different shapes and dimensions, which provide them with a great potential in the vast scope of applications. PVDF polymers have four phases; alpha, beta, theta, and gamma. However, only the beta phase has the potential usage in the applications because of its piezoelectric property (Salimi and Yousefi 2003, Zhu, Zeng et al. 2008). Lately, PVDF is used in tissue engineering application as a scaffold.

2.8 PVDF Scaffold

The scaffold provides mechanical support to the tissue during the recovery period. Host cells can attach to the scaffold, and that provides the tissue with an environment to populate and develop subsequent tissue (Lannutti, Reneker et al. 2007, Chan and Leong 2008). Polymeric biomaterials, which are biocompatible with enough mechanical strength, are being used to produce scaffolds. Moreover, for robust tissue growing, they have sufficient surface area and porosity. Electrospun scaffold eliminates these drawbacks and performs the way that is needed (Sakaguchi, Amoroso et al. 2014).

Certain piezoelectric materials can be employed as a scaffold for supporting the nerve regeneration process. Due to their biocompatibility and piezoelectric properties, PVDF is one of the ideal polymers that can perform as a scaffold. Piezoelectric polymers can electrically stimulate the tissue when mechanical deformation occurs. Generated electricity helps the nerves regenerate (Halabi, Behrens et al. 2014). It has been shown

that PVDF-TrFE scaffold has induced recovery of cardiovascular cell types (Hitscherich, Wu et al. 2016).

2.9 Application of Piezoelectricity

Ferroelectric crystals are the core in most of the commercial piezoelectric materials. BaTiO₃ was the first commercially manufactured piezoelectric material (Barsoum 1997). Detection of mechanical vibrations, producing charge at high voltages, control of frequency, and generation of ultrasonic and acoustic vibrations are the most common reasons that piezoelectric materials are being used for. Sensors and actuators are manufactured by using bulk ceramics which are formed into common shapes. For ultrasonic imaging, thermal imaging, pollution sensors, and microphone applications plates, cylinders, and blocks are employed (Kasap 2002).

Piezoelectric materials are the milestone for Micro-electrical-mechanical-system (MEMS) applications. MEMS is a relatively new and breakthrough technology for the circuit industry. Thanks to this technology, it is possible to produce smaller devices. In spite of the small structure of these new devices, their productivity is equal and higher compared to bulk materials. Furthermore, MEMS enables the industry to produce lower cost materials (Peterson 1998).

The ultrasonic medical applications are the other relevant field for utilization of piezoelectric materials. There are many advancements of ultrasonic diagnostic tools in recent years. The main advantage of using ultrasonic imaging is that it can make minimally-invasive surgery possible. This technique is safer and provides surgeons to distinguish between soft tissue and organs. Soft PZT ceramics are also widely used in medical imaging (Schwartz 2003).

2.10 Piezoelectric Actuators

Actuators and sensors make systems smart and adaptive. Smart materials understand the environment and can respond to the external stimulus without any need for human intervention. The main mechanism of operation for smart materials is converting one energy form to another. Piezoelectric and electrostrictive devices have become key components in smart actuator systems such as precision positioners, miniature ultrasonic motors and adaptive mechanical dampers. When an electrical field is applied to piezoelectric materials, there are two main kinds of behaviors that may occur in the material. First one is that the thickness of the material will increase. This kind of bending behavior is observed on piezoelectric stack actuators. Second behavior is called planer motion. The electrical field causes the plate to move to a planer contraction, under the above conditions. This behavior is used for piezoelectric bending actuators. A substrate sheet and the PZT-layer are contained in bending actuators (Qing-Ming, Xiao-Hong et al. 1999).

2.11 Longitudinal Actuators

In longitudinal piezoelectric actuators, the electric field is applied parallel to the ceramic layer's polarization direction. This causes a displacement or strain in the way of polarization. Despite the fact that individual layers produce small displacements only, aggregate displacement is much higher because the stack actuator consists of many layers (Figure 1.11). Longitudinal stack actuators are highly efficient in converting electrical energy to mechanical energy.

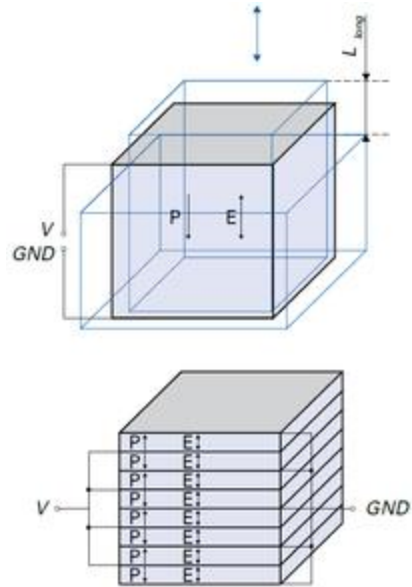


Figure 2.6 Longitudinal displacement (top) and polarization of the individual layers (bottom) of a stack actuator.

Estimation of the longitudinal displacement where:

$$\Delta L_{long} = n d_{33(GS)} V \quad (2.8)$$

CHAPTER 3

RESEARCH DESIGN AND METHODOLOGY

3.1 Overall System Description

As mentioned in Chapter 2, piezoelectric materials generate an electrical output when they are subjected to mechanical stress. In this design, a mechanical strain is applied to the piezoelectric material to be tested. Concurrently, the output is collected through the data acquisition (DAQ) board. Figure 3.1 shows the general setup of the system, and the data flow.

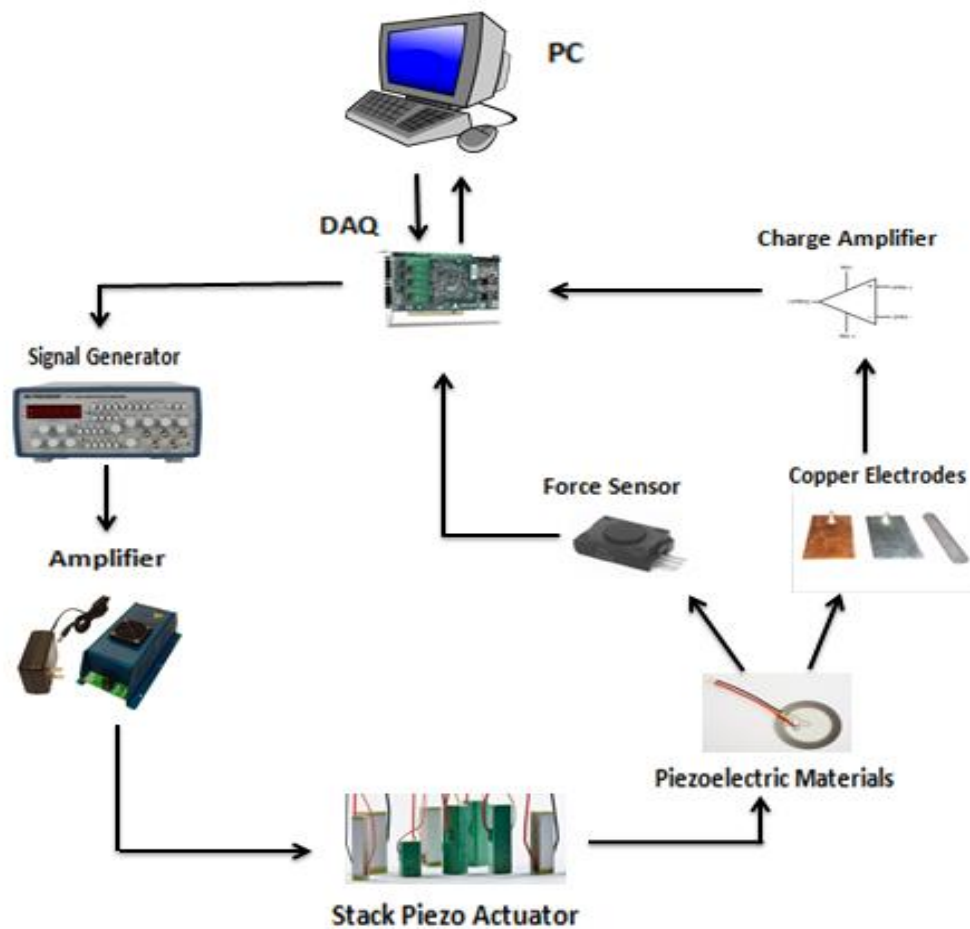


Figure 3.7 Block diagram of data acquisition for applying stress to the piezoelectric material and collecting the data into the computer via the NI DAQ Board.

In this block diagram, it can be seen how data is flowing. First, in the computer, the user can produce a waveform and set its amplitude, frequency, and duty cycle. The DAQ board sends this waveform to the signal generator and the signal generator produces the desired waveform. After generating this signal, it is amplified because in order to drive stack actuator, a high voltage source is needed. Stack actuator receives the generated signal and produces force. Upon applying the force, the piezoelectric material under testing generates electricity, and the voltage difference between the two sides of the material is detected by the copper plates. Since piezoelectric materials produce charge, a charge amplifier is used to collect this charge, integrate, and amplify it. Then for signal processing, the amplified signal is sent to a desktop computer through the DAQ board. Finally, the results are analyzed in Matlab.

A force sensor is also added to the system and the applied force and the piezoelectric material's response are collected simultaneously into the computer. With this setup, materials can be characterized by comparing the applied force and the output voltage from the material being tested.

3.2 DAQ Board

Only two inputs and one output channels of the NI PCI 6259 DAQ board are needed in this study. One of the inputs is connected to the amplifier that amplifies the signal coming from the copper electrodes (plates). The other input is connected to the force sensor. The DAQ board output is connected to the signal generator to produce the control signals.



Figure 3.8 NI PCI 6259 DAQ Board, maximum sampling frequency is 1.25 MHz.

Source: NI datasheet. 2014, November 06. Retrieved from <http://sine.ni.com/nips/cds/view/p/lang/en/nid>

3.3 BK Precision Signal Generator

In order to give voltage to the stack actuator, BK Precision 4040A signal generator is used. It has a wide frequency range that allows the user to apply different frequencies to the stack actuator. The other important feature is that several different signal waveforms can be applied to the actuator such as square, sinusoidal, or triangle wave and different force patterns can be obtained easily. Moreover, if it is needed, the duty cycle of the waveform can be varied through the computer by taking advantage of a control input available on this signal generator. The signal generator has a 0.2 Hz to 20 MHz frequency range.



Figure 3.9 BK Precision Signal Generator.

Source: Retrieved from <http://www.bkprecision.com/products/signal-generators/4040A-20-mhz-sweep-function-generator.html>.

3.4 Amplifier

It is because the stack actuator needs a high excitation voltage to function, a voltage amplifier is used to magnify the control signal that is produced by the signal generator. The EPA-008 is a high voltage linear amplifier with an integral high voltage power supply. It is designed to be small in size and convenient for bench top experimentation. It accepts a +/- 10 V_{peak} ground referenced input signal and produces a +/- 180 V_{peak} ground referenced output drive signal. It is designed to be used as a high voltage drive source for various piezoelectric actuating devices operated from DC to the low audio frequency range. (EPA-008-1 datasheet)



Figure 3.10 EPA-008-1 Linear Amplifier.

Source: Retrieved from <http://www.piezo.com/prodelect2epa008.html>.

3.5 Charge Amplifier

A charge amplifier produces a voltage output which is proportional to the integrated value of the input current. When piezoelectric materials are under mechanical stress, they will produce electrical charges. However, under the static stress, due to the internal resistance of the piezoelectric material, the produced charge will decay over time. The charge amplifier collects the charge before it discharges to ground and stores it in a capacitor and maintains a voltage that is proportional with the collected charge.

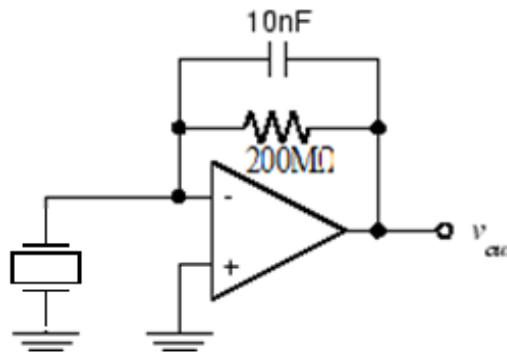


Figure 3.11 Charge amplifier circuit.

3.6 Force Sensor

The FS03 force sensor is used to measure the applied force to the piezoelectric materials. The FS03 sensor is a low cost, piezoresistive-based force sensor. It is employed in this design because it has a high-level voltage output, calibration, and temperature compensation sensor, which gives an accurate and stable output over a 5 °C to 50 °C [41 °F to 122 °F] temperature range. Operation from any DC supply voltage, up to 12.0 Vdc, is acceptable. Their small size enables the use of multiple sensors in limited space. (FS03 datasheet)



Figure 3.12 FS03 Force sensor.

Source: FS03 datasheet.

3.7 Stack Piezoelectric Actuator

Stack piezoelectric actuators are used as linear electromechanical drivers or motors. They act mainly like an expanding element generating a compressive force. The complete motion cycle is nearly proportional to a voltage signal input from DC up to high frequencies. It has a compact size, accurate positioning in nm, high-speed response and large blocking force. Also, it is easy to be controlled by a voltage source. (Stack actuator datasheet)

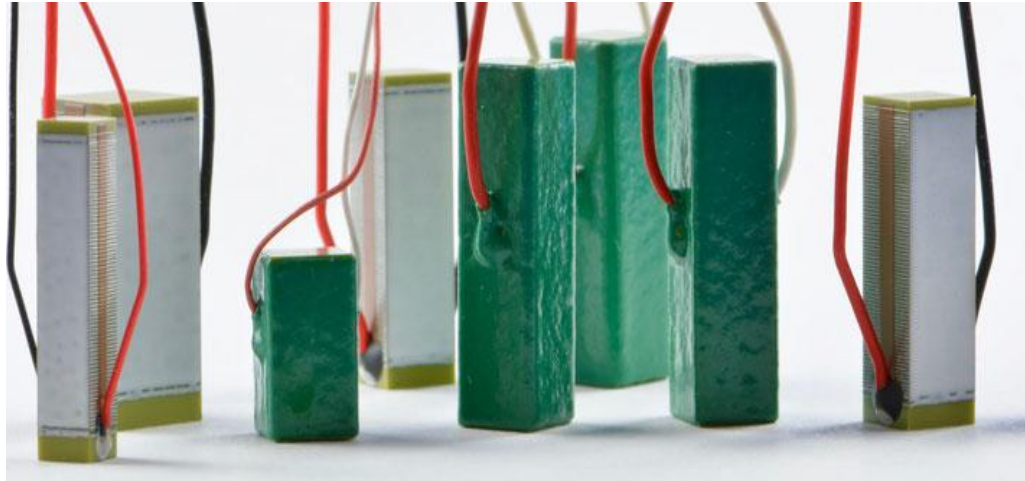


Figure 3.13 Piezoelectric stack actuator.

Source: Retrieved from <http://www.piezotechnics.com/>

3.8 Faraday Cage

A Faraday cage is an enclosure container made by conductive mesh wire or plates. Not every piezoelectric material generates a high output voltage. Therefore, if there is noise during data acquisition, which will contaminate the investigated signal. Faraday cage is used to reduce noise, especially the 60 Hz noise from the power lines, and ensure a high quality signal even with low output voltages. It is almost impossible to eliminate all noise from the system, but it can be minimized by using a Faraday cage and some other noise cancellation techniques. Depending on the recording environment, the electrodes, which can be metal needles and wires, can pick up electromagnetic waves, or other types of electrical noise. A Faraday cage can be used to prevent most of these noise sources.



Figure 3.14 Faraday cage.

Source: Retrieved from <http://www.scientifica.uk.com/product.php?shopprodid=102>.

3.9 Experimental Procedure

In this system, as mentioned in Section 3.1, a mechanical stress is applied to the piezoelectric materials by using piezoelectric stack actuator. Thanks to the stack actuator, different waveforms and frequencies can be produced and applied to the materials under testing.

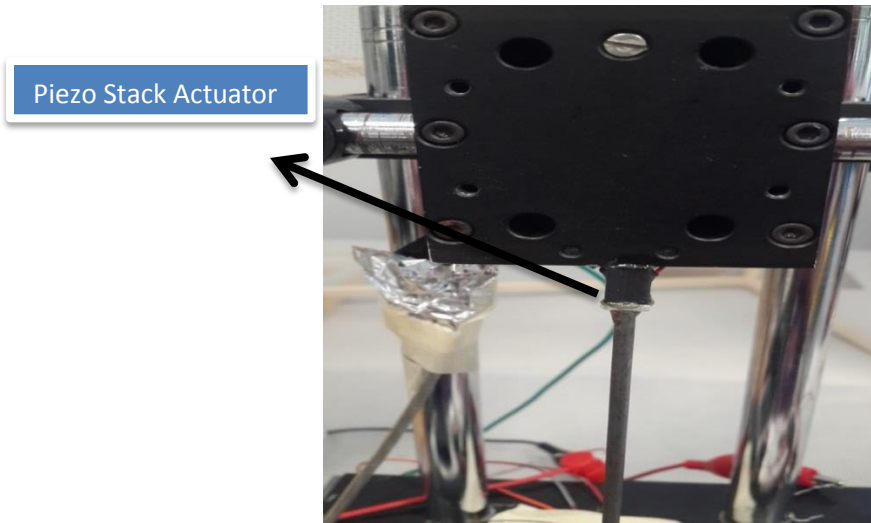


Figure 3.15 Piezoelectric stack actuator.

The stack actuator is glued to a micromanipulator which helps to arrange the initial position of the stack. Moreover, the initial, steady force can be controlled by using the micromanipulator.

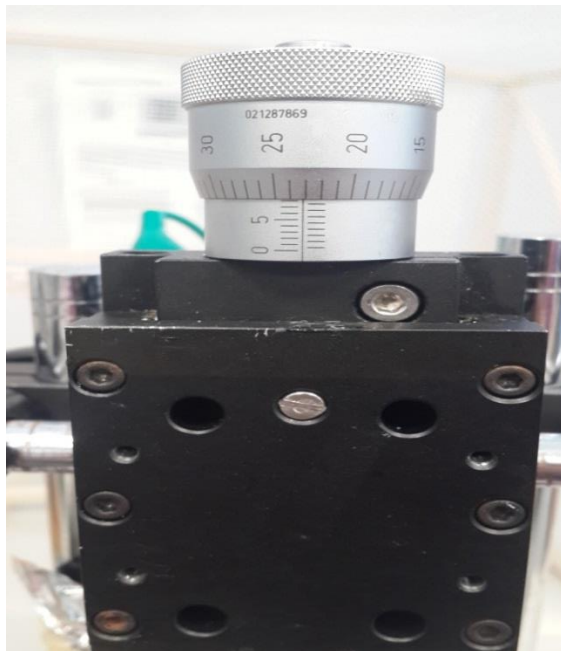


Figure 16 Micromanipulator.

There is a metal stick that was glued to the stack actuator to transfer the stress to the material and the force sensor. The stack should not be directly placed over the piezoelectric material and force sensor, because it is being driven by a high voltage, and this high voltage can cause substantial electrical artifact on the recorded signal.

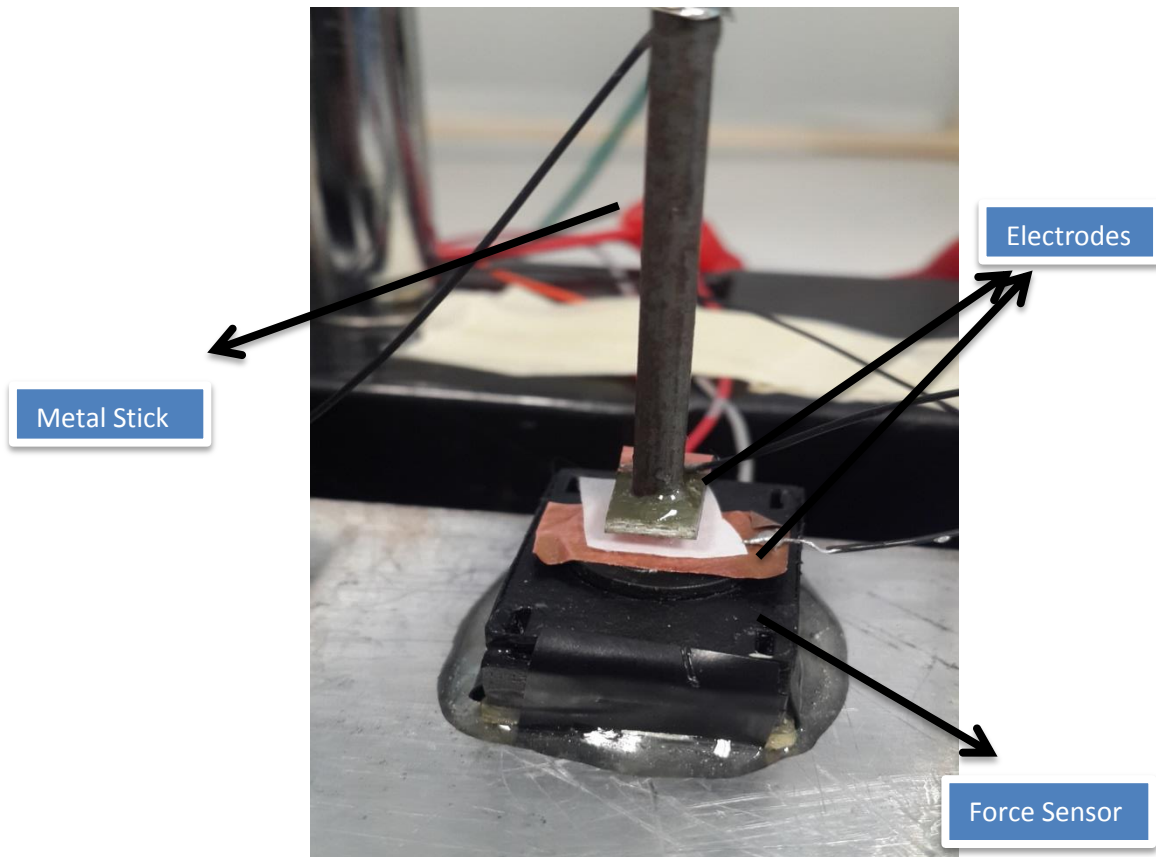


Figure 3.17 Electrodes and force sensor.

On the other side of the stick, one of the electrodes is glued to the stick and also the stick is grounded to prevent any potential noise. In addition, another copper electrode is placed on the force sensor, hence the applied force and output voltage from the piezoelectric materials can be measured at the same time. The force sensor output is directly connected to the DAQ board; concurrently, the piezoelectric material's output is connected to the charge amplifier.

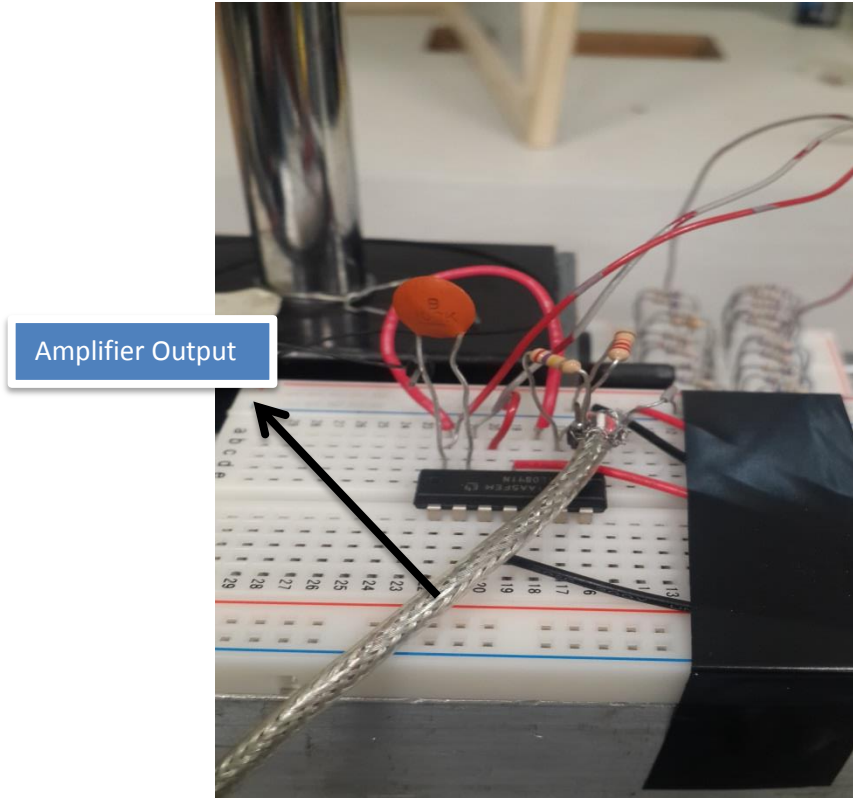


Figure 3.18 Charge amplifier.

After the amplification, the output voltage is connected to the DAQ board. The signal generator is used to drive the stack actuator. Since the input of the stack can go up to 150 V, an amplifier is needed to amplify the signal generated by the signal generator.

To prevent any noise contamination, everything is grounded in the system, and the Faraday cage is used to eliminate 60 Hz and any other electromagnetic threat. After collecting data, the data is analyzed on the computer in Matlab, and based on the results, the materials can be characterized for their piezoelectric properties.

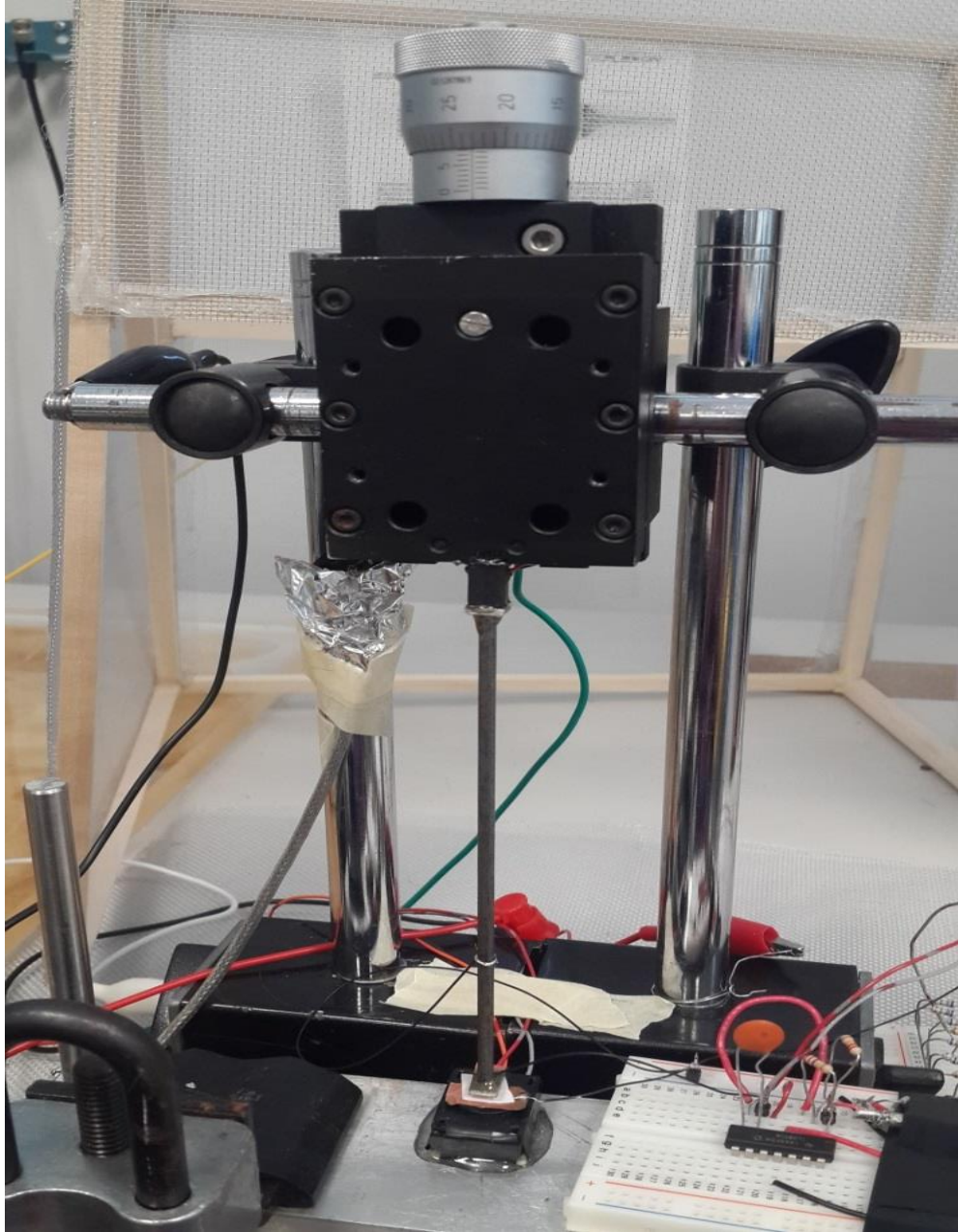


Figure 3.19 General view of the design.

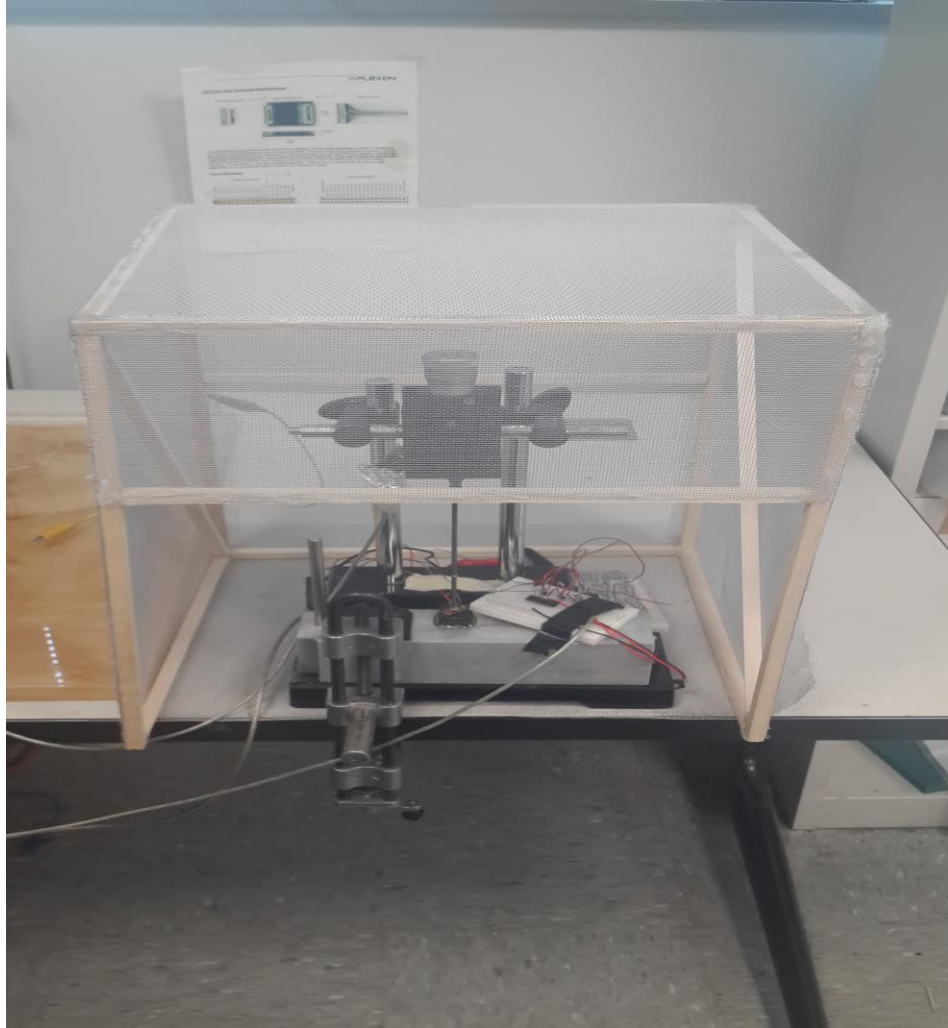


Figure 3.20 General view of the design with the Faraday cage.

CHAPTER 4 RESULTS and DISCUSSION

4.1 Stack Piezoelectric Actuator Response to Varying Voltages

There are two ways to control the force applied to the material under testing. The first one is using the micromanipulator to apply a constant compression. This helps the user to adjust the baseline force. The second approach, also used during data collection, to control the applied force is by adjusting the stack actuator's voltage level. During data collection 20V, 40V, 60V, 80V, 100V, 120V, 140V, and 150V are applied to the stack actuator. It is important to consider that 150V is the maximum value that can be applied to the actuator according to the datasheet. The figure below indicates this relationship.

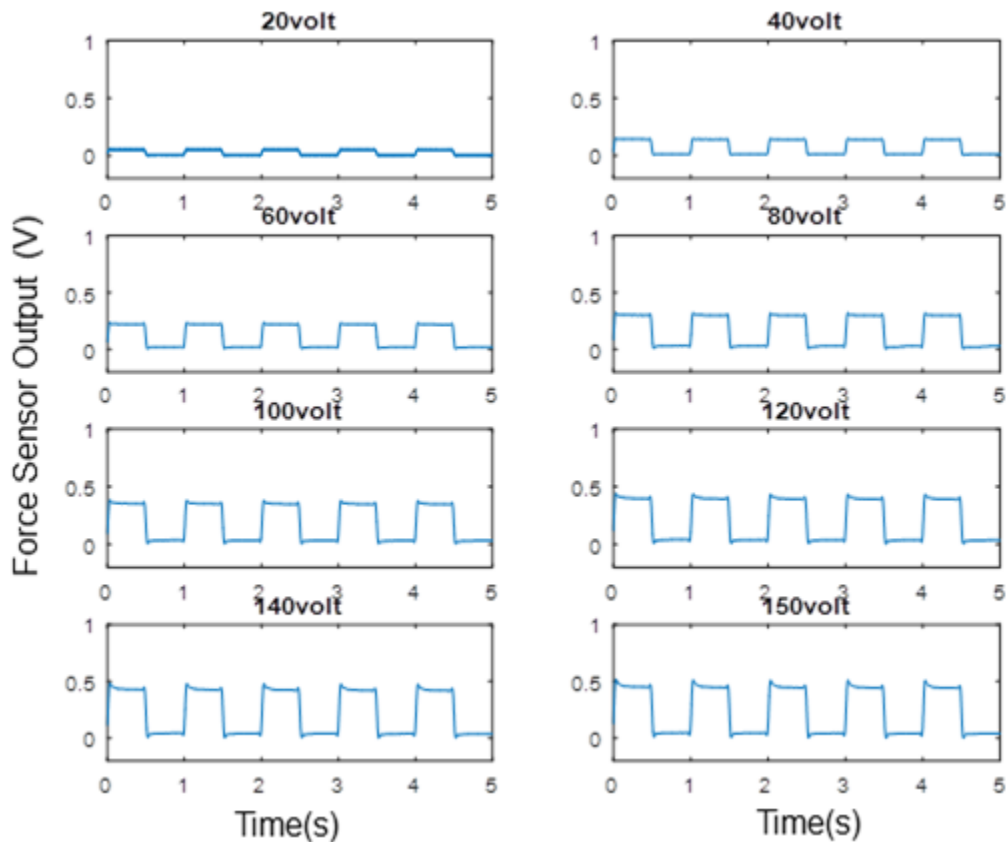


Figure 4.21 Output voltage of the force sensor at increasing voltages applied to the

piezoelectric actuator. The signals are filtered with a low-pass filter on the computer for clarity of presentation.

In order to convert the force sensor output (V) to Newton (N) units, the following formula that is given in the force sensor datasheet was used:

$$Output(V) = \frac{0.8 \times V_{supply}}{Force_{range}} \times (Force_{applied}) + 0.01 \times V_{supply} \quad (4.1)$$

The Figure 4.2 was obtained by applying Equation 4.1 to the previous results. Observing the relationship obtained between the stack actuator output force and the applied voltage to the actuator, we can conclude that these measures are directly proportional. Hence, increasing the applied voltage to the actuator causes proportionally larger output forces.

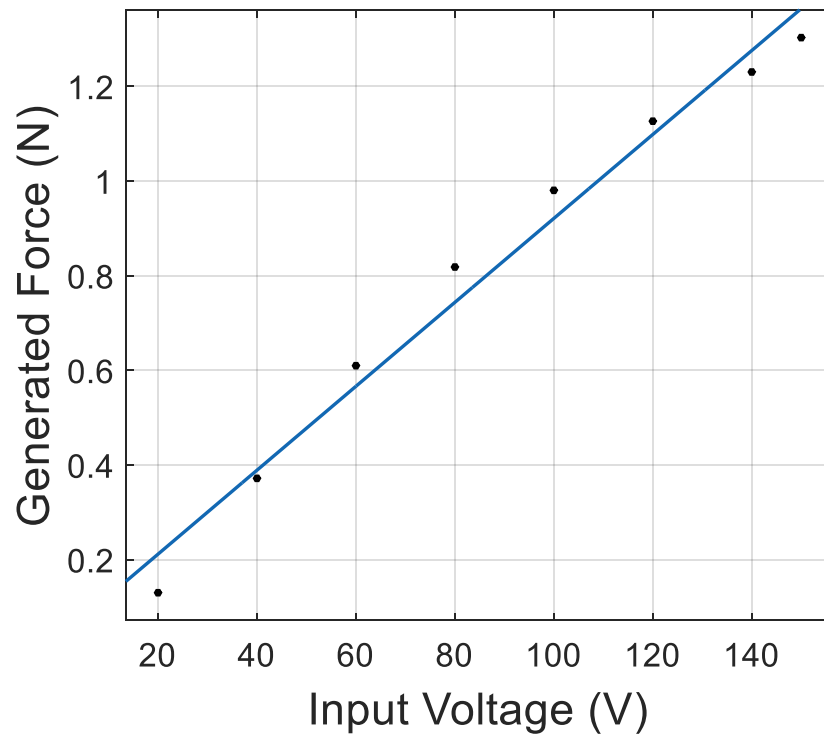


Figure 4.2 Correlation of the generated force by actuator and actuator's input voltage.

The following linear model shows the relationship between these two measures.

Linear model Poly1:

$$f(x) = p1 * x + p2 \quad (4.2)$$

Coefficients (with 95% confidence interval):

$$p1 = 0.008868 \text{ (0.007611, 0.01013)}$$

$$p2 = 0.03443 \text{ (-0.0901, 0.159)}$$

Goodness of fit:

SSE: 0.02453

R-square: 0.98

Adjusted R-square: 0.977

RMSE: 0.06394

Considering the outcomes of the analysis, and observing an R-square value of larger than 0.95 to a linear line fit, we can conclude that the observed data indeed follows a linear trend.

4.2 Stack Piezoelectric Actuator's Response to Various Waveforms

Several types of waveforms are applied to the stack actuator to investigate if the waveform will be maintained on the force sensor's output. The results can be seen in figure 4.3.

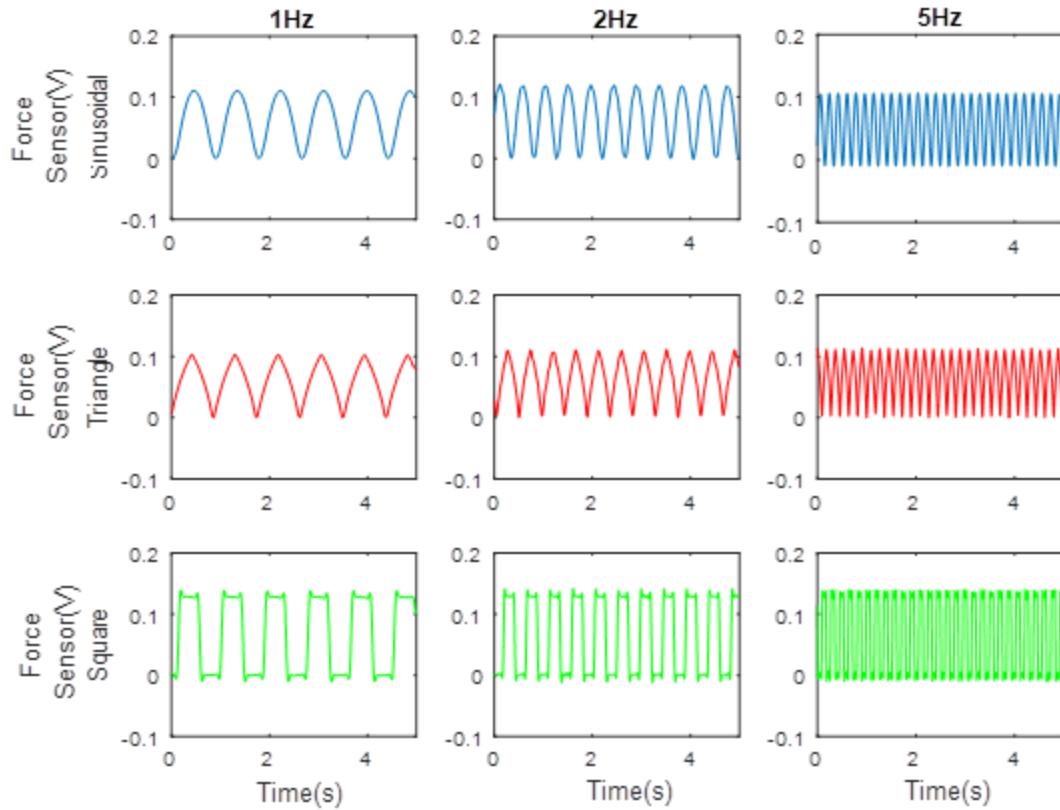


Figure 4.3 Force sensor output to different waveforms applied to drive the stack actuator.

Figure 4.3, corroborates that the stack actuator can follow different waveform types of the driving voltage with a close representation of the signal in the generated force. Slight deviation from the original waveform occurs due to the lack of very high frequencies as this will be demonstrated in the next section.

4.3 Sinusoidal Excitation of the Stack Actuator

Figure 4.4 illustrates the piezoelectric stack actuator's peak-to-peak force output at different frequencies of the driving voltage with a sinusoidal waveform.

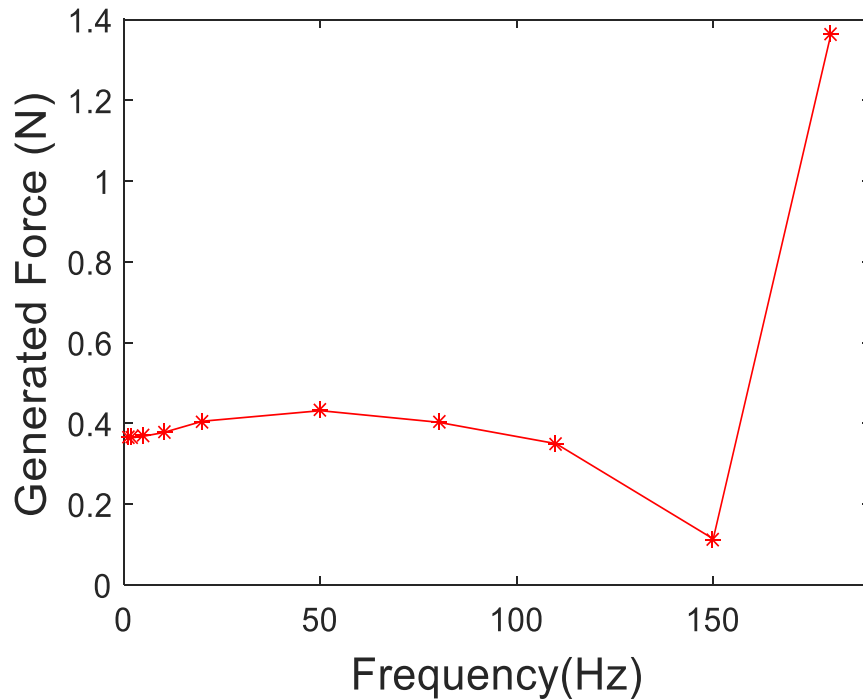


Figure 4.4 Measured peak force at different frequencies of sinusoidal waveform.

The amplitude of the mechanical stimulus was kept constant, only the frequency of the signal was varied in the range of 0-200Hz. As observed in Fig. 3.5 the actuator's output force is frequency dependent. Up to 100Hz, the actuator's force is more or less constant with a slight peak around 50Hz. Around 150Hz, there is dip in the output force before it starts increasing again. The actuator gives the highest response at 180Hz, which is the resonance frequency for this particular device as specified in its datasheet.

4.4 Metallic PVDF Measurement

To test the system, measurement were made using commercial PVDF material (by Goodfellow Inc.) with both sides coated with metallic film. Different voltages were applied to the stack actuator, and the generated force was applied to the PVDF. The

applied force was measured by the force sensor. After collecting data, the voltage output of the force sensor was converted to Newton (N) based on the given equation by the force sensor's manufacturer.

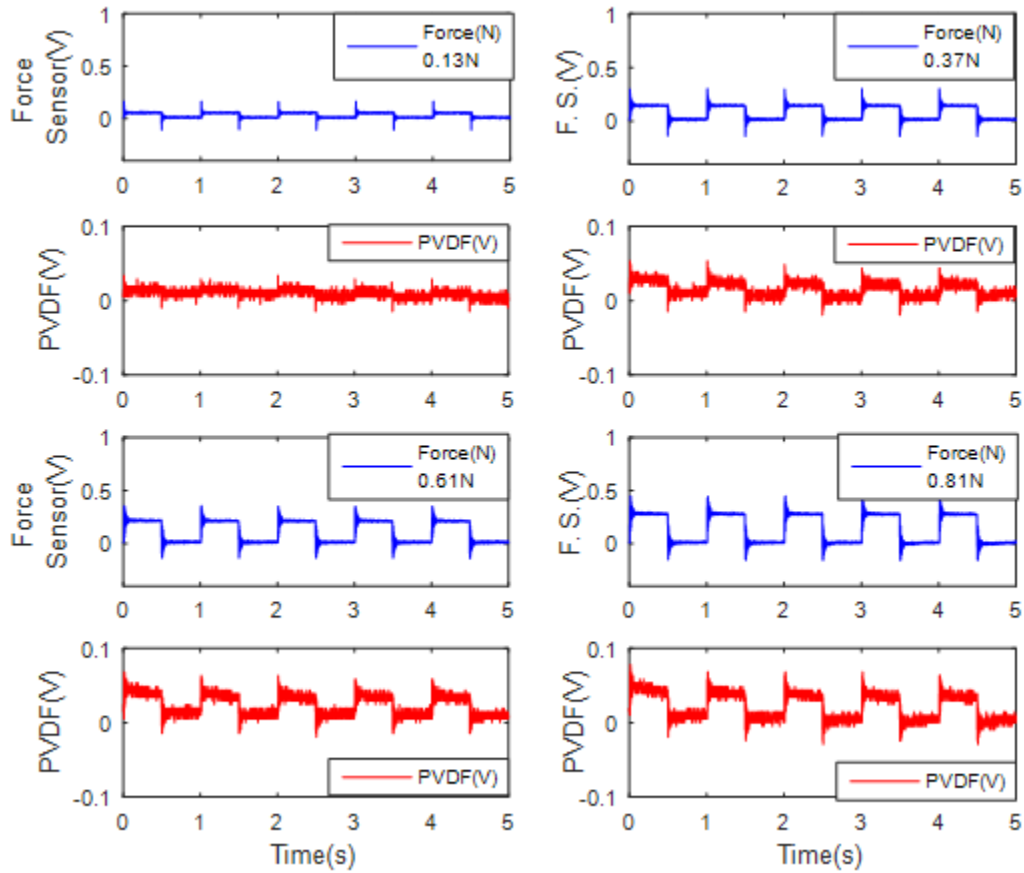


Figure 4.5 The PVDF response at different force amplitudes varied between 0.13N and 0.81N. Applied force is a 1 Hz square wave.

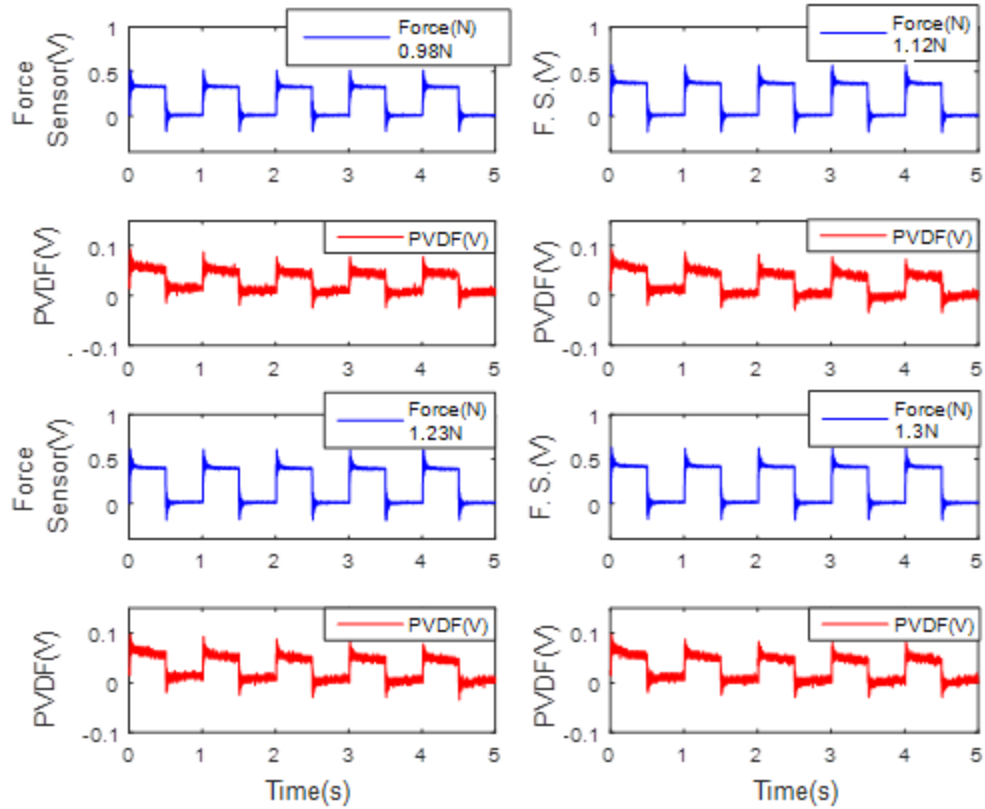


Figure 4.6 The PVDF response at different force amplitudes varied between 0.98N and 1.3N. Applied force is a 1 Hz square wave.

Before converting the output voltage to Newton, raw data is filtered with a low-pass filter. The filter has sixth order, and the cutoff frequency is 10Hz. After filtering the signal, the equation is used to convert the voltage to Newton. Considering that the second input comes from the PVDF output, the output should be converted to surface charge density since it is the amplified output. The formula for conversion is showed below.

$$Q=C*V \quad (4.3)$$

The voltage (V) is calculated from the amplitude of the output signal, and the capacitance (C) is 10nf as shown in the charge amplifier's schematic. After applying the formula for conversion, we should indicate that there is a non-inverting amplifier, and its gain factor

is 12. Thus, the resulting value (Q) needs to be divided by 12. In order to find the charge (coulomb) per millimeter square, the last calculated, Q, value is divided by the area, $5\text{mm}\times 7\text{mm}$, over which the force was exerted. The unit of the final value is C/mm^2 .

In order to understand the relationship between the force and the PVDF output, the following graphic was produced:

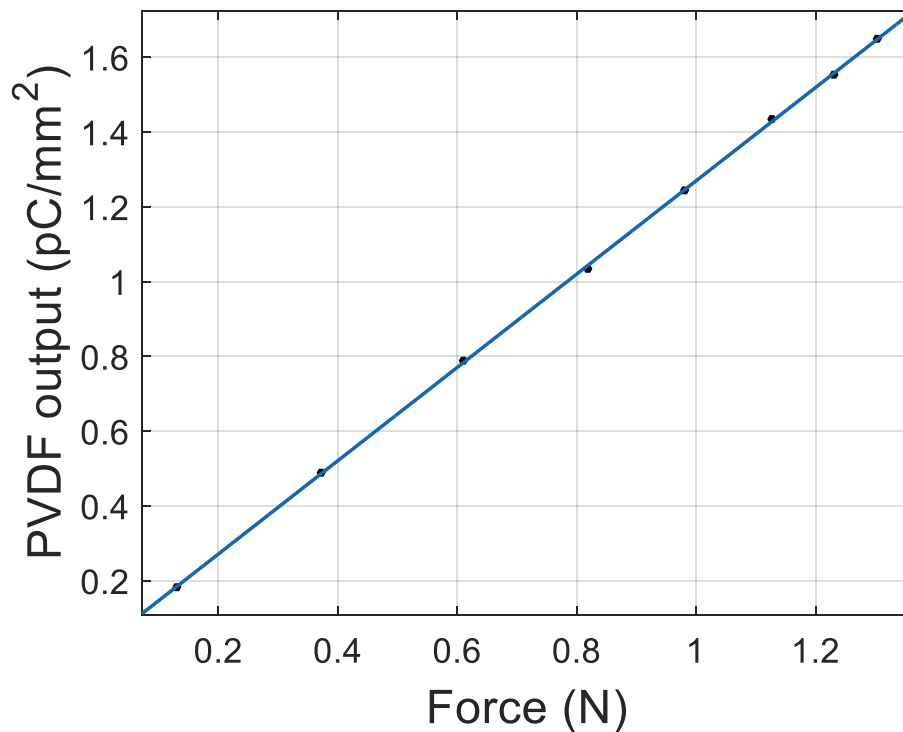


Figure 4.7 A linear line fit to the PVDF output data. Applied force is a 1 Hz square wave.

Once again, we can see that the values show a linear relation that we are seeking to prove.

Figure 4.7 was obtained using the average of 5 different samples, and it shows the relationship between output voltage of the piezoelectric PVDF and applied force. The X axis represents the change of the applied force, and the Y axis indicates the output of the

PVDF. As it can be seen in the figure, PVDF output and applied force seem to have a directly linear relation. The following linear model shows the relationship between the force and the PVDF material.

Linear model Poly1:

$$f(x) = p1*x + p2 \quad (4.4)$$

Coefficients (with 95% confidence bounds):

$$p1 = 1.247 \quad (1.235, 1.26)$$

$$p2 = 0.0223 \quad (0.01098, 0.03362)$$

Goodness of fit:

SSE: 0.0001923

R-square: 0.99

Adjusted R-square: 0.99

RMSE: 0.005662

As the results show, the R-square and the adjusted R-square of this model are above 0.99 which indicates that the relationship between the applied force and the PVDF material is indeed highly linear.

D_{33} value, 43.64×10^{-12} , is found by dividing produced charge to applied force. When calculated value is compared to the d_{33} value from datasheet, 20×10^{-12} , a slight difference is observed. The reason may result from electrodes quality.

4.5 PZT Measurements

As a second material of choice, another piezoelectric material, PZT (by Piezo System Inc.), is tested. The force vs. output voltage relationship of the PZT is shown in Figure 4.8. The main difference between this data and the previous one is the fact that this time a sinusoidal signal is applied to the actuator.

Once again the relationship seems to be linear.

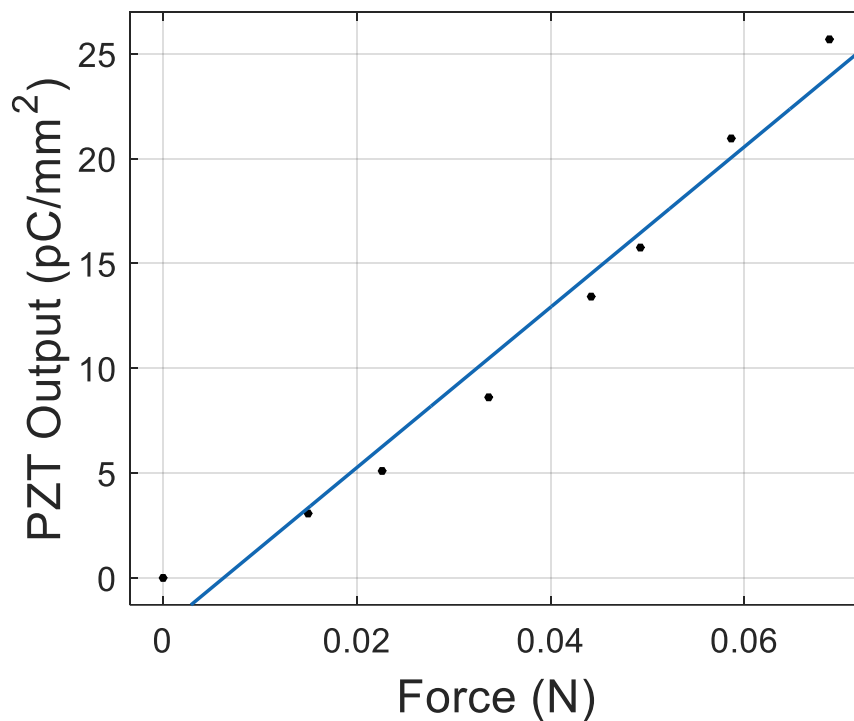


Figure 4.8 The PZT output voltage vs. the force. Applied force frequency is 1 Hz.

Figure 4.8 shows the relationship between the output voltage of the PZT and the applied force. The X axis represents the applied force, and the Y axis shows the output of the PZT. As seen in the figure, the PZT output and the applied force seem to have a linear relation. The following linear equation was used to model the relationship between the force and the PZT material.

Linear model Poly1:

$$f(x) = p1*x + p2 \quad (4.5)$$

Coefficients (with 95% confidence bounds):

$$p1 = 382.5 \quad (316.9, 448.1)$$

$$p2 = -2.387 \quad (-5.173, 0.3986)$$

Goodness of fit:

SSE: 16.19

R-square: 0.9714

Adjusted R-square: 0.9666

RMSE: 1.643

As the result shows, the R-square and the adjusted R-square of this model are above 0.98 which indicates that the relationship between the applied force and the PZT material is indeed linear.

D_{33} value, 127.3×10^{-11} , is found by dividing produced charge by force. When compared to d_{33} value from datasheet, 390×10^{-12} , the measured value is three times larger. The discrepancy may result from the sample sizes used by us and the manufacturer. The company may also be reporting the minimum charge values that are guaranteed in a randomly chosen sample.

When a sinusoidal signal is applied to the stack, the output of the PZT maintains the shape of the signal to a large extent, as shown in the figures below.

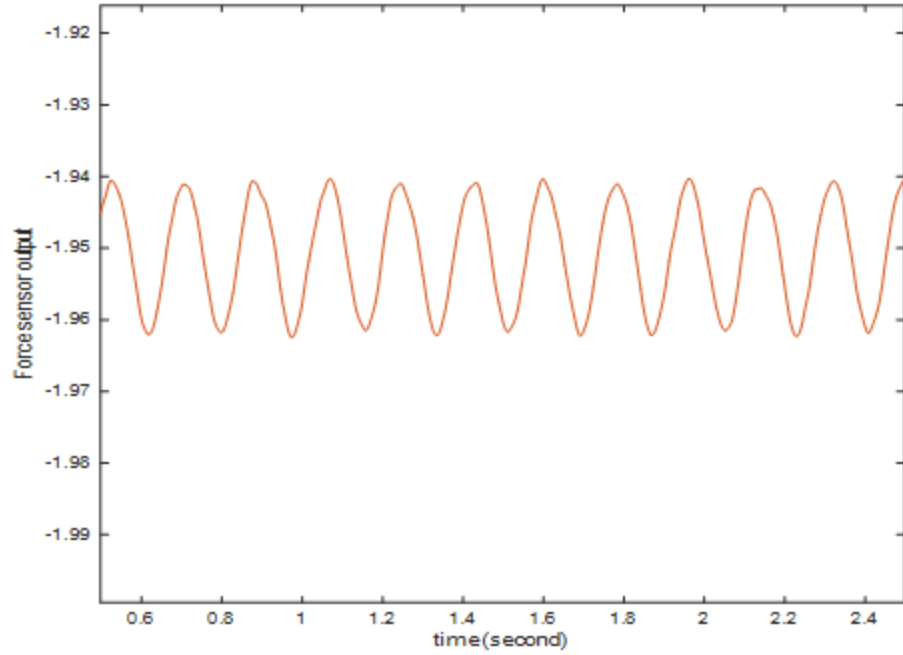


Figure 4.9 Force sensor output.

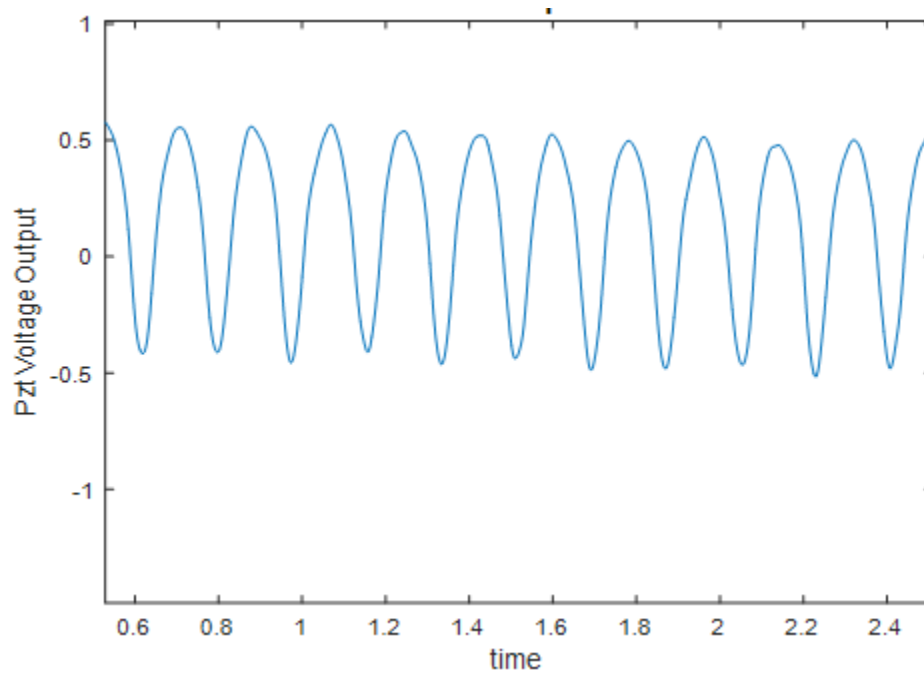


Figure 4.10 PZT output. Applied force frequency is 5 Hz.

In addition to these results, it could be observed that PZT has higher output response compared to PVDF. Even under a low force, it gives much higher voltages than PVDF.

4.6 Non-Piezoelectric Material Measurement

As a control, a non-piezoelectric material was tested, and its output was compared with that of the PVDF material. Figure 4.11 shows the impact of the force on the non-piezoelectric material.

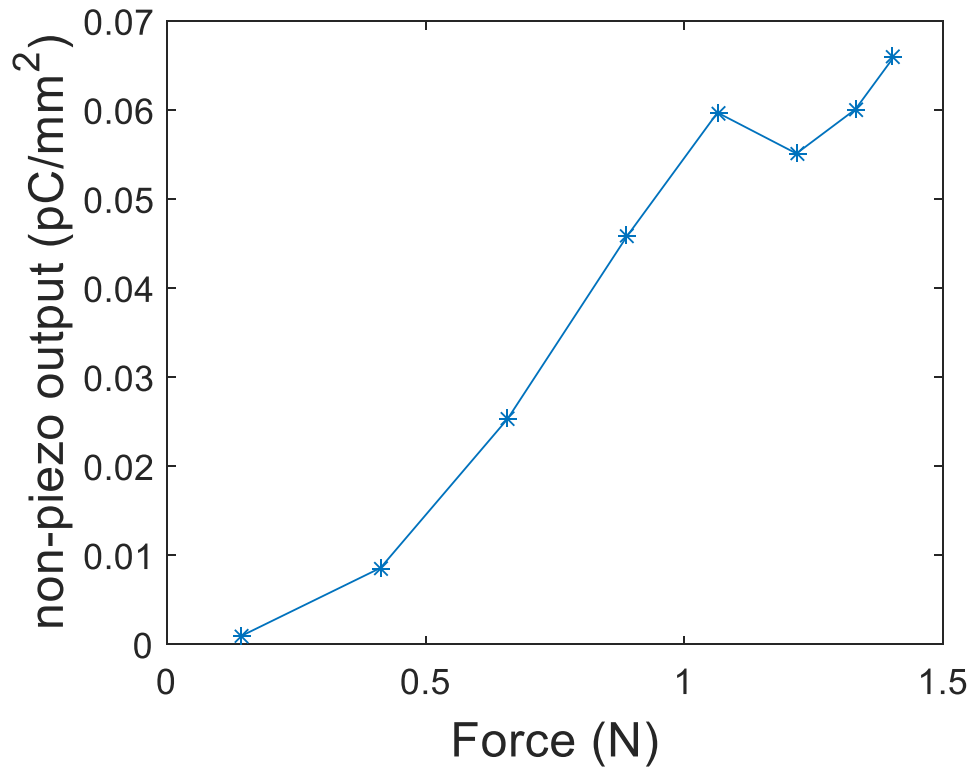


Figure 4.11 Relationship with force non-piezoelectric material output. Applied force frequency is 1 Hz.

Once the control test was finalized, we needed to relate these results to the ones obtained from the PVDF experiment. The results of this comparison are shown in the Figure 3.12.

4.7 Piezoelectric vs. Non-piezoelectric

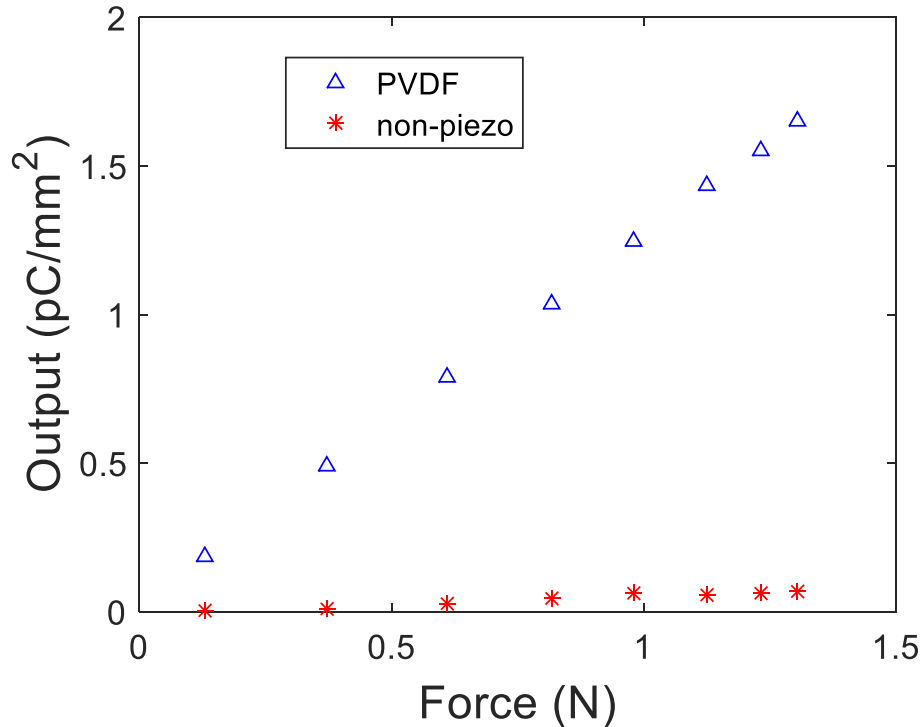


Figure 4.22 Comparison between PVDF film and non-piezoelectric material's output.

Figure 4.12 shows the difference between the piezoelectric and non-piezoelectric materials. This control phase shows that the PVDF material clearly produces an output voltage compared to non-piezoelectric materials, which also indicates that there is some amount of noise in the system. The reason for the output voltage with the non-piezoelectric material can be the capacitance change across the material under mechanical perturbations, electrical crosstalk from the actuator driving voltage, or the motion artifact.

4.8 Design Comparison

In order to assess this system's pros and cons, some commercially available

designs are investigated. For instance, Piezotest Inc. is one of the well-known companies working on characterization of piezoelectric materials. Their product, D33 Piezometer device, is capable of applying forces at varying frequencies, from 30 Hz to 300 Hz. However, it is not able to implement different waveforms of the force. Another piezo test meter device manufactured by Sinocera Piezotronics Inc. can comparatively produce low forces, 0.25N, to apply to the materials under testing. Unlike commercial devices, the designed setup in this study is capable of applying higher forces with frequencies adjustable from DC to 200 Hz. Furthermore, different force waveforms can be implemented. Also, with a small modification, the system can begin testing piezoelectric materials in wet conditions, which is a necessary step for better understanding how PVDF scaffolds behave *in vivo*.

CHAPTER 5

CONCLUSION AND FUTURE WORK

5.1 Conclusions

This study was set out to design an electromechanical system to characterize the piezoelectric property of the materials. Piezoelectric materials have such exquisite characteristics in responding to mechanical stimulations by producing electrical output. Converting one energy type to another makes them exceptional and beneficial for both therapeutic and diagnostic purposes. Tissue recovery, piezosurgery, and pressure sensing are some of the areas where piezoelectric materials find applications in medicine.

In this study, an electromechanical system is designed to investigate the piezoelectricity of such materials. First, varying levels of mechanical stress can be applied to the materials to obtain the force-voltage relationship. This relationship also provides necessary calibration information to compare with different piezoelectric materials. Second, the response of the piezoelectric material at different waveforms of the mechanical stimulus can be determined using the system developed. Finally, the mechanical stimulus frequency can be adjusted within a desired range to evaluate the material's response as a function of frequency. Understanding their frequency limitation is important for their intended purpose since the response may get distorted at high frequencies.

In order to produce mechanical perturbations as described above at various frequencies and waveforms, a piezoelectric stack actuator is used. As a piezoelectric device, stack actuator is producing mechanical stress when it is under the effect of

electricity, which is the indirect effect. The produced force by the stack actuator can easily be controlled by adjusting the exciting voltage. Moreover, it has a steady response both at relatively high frequencies and with different waveforms.

In order to test the system, piezoelectric materials PVDF and PZT, and a non-piezoelectric material are utilized. Figure 4.15 shows the PVDF and non-piezoelectric material response to the same applied force. Also, the PZT's sinusoidal signal response can be seen in Figure 4.13. This study provides a straightforward way to analyze and test piezoelectricity of the materials.

The main difficulty in this study was finding a way for applying different mechanical strain at various waveforms and frequencies under one design. After designing various setups, we decided to use a piezoelectric stack actuator. Another important design challenge was elimination of noise from the recordings. To do this, a Faraday cage was custom-made, and all metal parts in the system were grounded. To prevent motion artifact, the system was firmly fixed with mechanical parts. Also, for the electrical artifact, a metal stick was used to move the high-voltage-driven stack actuator away from the recording area.

5.2 Future Work

For further studies, an actuator with a larger force rating can be employed to obtain higher mechanical stress. Also, to investigate the material's response under different conditions, such as in dry and wet media, some modifications needs to be implemented on the design. That is, if it needs to be studied how implanted piezoelectric materials

behave in the body, especially with PVDF scaffolds, a wet environment can mimic the *in vivo* situation more realistically.

APPENDIX

MATLAB CODES

Data Acquisition Codes

```
clear

tic

ai = analoginput('nidaq','Dev2');

ai.ClockSource = 'Internal';

ai.BufferingMode = 'Auto';

ai.TriggerType = 'Immediate';

ao = analogoutput('nidaq','Dev2');

ao.ClockSource = 'Internal';

trial =3; % number of trials

daqfile = ['trial' num2str(trial) '.daq'];

ai.LogFileName = daqfile;

ai.LogToDiskMode = 'index';

ai.LoggingMode = 'Disk&Memory';

ai.InputType = 'SingleEnded';

addchannel(ai,[20 21]);

addchannel(ao,[0]);

ActualRange = setverify(ai.Channel,'InputRange',[-10 10]);
```

```

set(ai,'RunTimeErrorFcn',@daqcallback)

set(ai,'ChannelSkewMode','Equisample');

duration =5; % duration of each trial/train in seconds

Fs=20000; % sampling frequency

ActualRate = setverify(ai,'SampleRate',Fs)

set(ai,'SamplesPerTrigger',duration*ActualRate);

set (ao, 'SampleRate', Fs)

f=1;

kj=0;

amplitude=50; % pulse amplitude

pulse_f=f; % pulse frequency in Hz

pulse_duration=500 ; % pulse duration in ms

num_pulses=duration*pulse_f;

PD=pulse_duration*0.001*Fs;

PInt=Fs/pulse_f-PD-1;

outdata=[0 amplitude*ones(1, PD) zeros(1, PInt)];

outdata2=[];

for i=1:num_pulses,

    outdata2=[outdata2 outdata];

end

```

```

outdata2=outdata2';

putdata(ao, outdata2);

start(ai);

start(ao);

data_trigger_time = ai.InitialTriggerTime

[data, time] = getdata(ai);

stop(ai);

stop(ao);

df=figure

t=1/Fs:1/Fs:duration;

plot(t,data(:,1))

hold on

plot(t,data(:,2),'r')

saveas(df,sprintf('forcestack(10)f%d.fig',f))

toc

```

Filtering and Converting

These codes for calculating force sensor output.

This repeated for each collected figure.

```
force_range=1.36;
```

```
vsupply=6;
```

```

a=openfig('sinus_5hz.fig');
b=findobj(a, 'type', 'line');
x_data=get(b,'xdata');
y_data=get(b,'ydata');
force=y_data;
time=x_data;
[b1,a1]=butter(3,10/(20000/2));
forcefiltered=filtfilt(b1,a1,force);
forcefiltered_new=forcefiltered(1:20000);
force_new=forcefiltered-min(forcefiltered_new)-0.01;
figure;
plot(time,forcefiltered);
q=findpeaks(forcefiltered);
a=size(q);
a=a(1,2);
w=findpeaks(-forcefiltered);
s=size(w);
s=s(1,2);
if a>s
    q=q(1:s)
elseif a<s
    w=w(1:a)

```

end

```
forcevalue(1)=mean(q+w);
```

```
applied_force(1)=((forcevalue(1)*force_range)/(.8*vsupply))*10;
```

Observed Material's Output

These codes perform to find charge density.

```
non_amplified=y_data/(270/22);
```

```
Q=(10-8)*non_amplified;
```

```
Q_per_mm=Q/(5.4*7);
```

```
Q_pico_per_mm=Q_per_mm/(10-12);
```

REFERENCES

- Bae, J.-H. and S.-H. Chang (2015). "Characterization of an electroactive polymer (PVDF-TrFE) film-type sensor for health monitoring of composite structures." *Composite Structures* 131: 1090-1098.
- Barsoum, M. (1997). "Fundamental of Ceramics." New York: McGraw-Hill Companies.
- Brown, L. F. (2000). "Design considerations for piezoelectric polymer ultrasound transducers." *IEEE Trans Ultrason Ferroelectr Freq Control*. Springer, New York, NY.
- Cady, W. G. (1946). "Piezoelectricity." Book.
- Chan, B. P. and K. W. Leong (2008). "Scaffolding in tissue engineering: general approaches and tissue-specific considerations." *European Spine Journal* 17(Suppl 4): 467-479.
- Devaraju, V. (2013). "Design, development and characterization of wideband polymer ultrasonic probes for medical ultrasound applications." Ph.D. Thesis, Drexel University, Philadelphia, PA.
- Eberle, G., H. Schmidt and W. Eisenmenger (1996). "Piezoelectric polymer electrets." *IEEE Transactions on Dielectrics and Electrical Insulation* 3(5): 624-646.
- Guinovart-Díaz, R., J. Bravo-Castillero, R. Rodríguez-Ramos, F. J. Sabina and R. Martínez-Rosado (2001). "Overall properties of piezocomposite materials 1–3." *Materials Letters* 48(2): 93-98.
- Haertling, G. H. (1999). "ferroelectric ceramics: History and Technology." *Journal of the American Ceramic Society*.
- Halabi, F. A., P. Behrens and B. Glasmacher (2014). "Application of electrospun piezoelectric PVDF-scaffolds for nerve regeneration." *Conference Paper in Biomedizinische Technik*
- Harrison, J. S. and Z. Ounaies (2001). "Piezoelectric Polymers." NASA Langley Research Center, Hampton, Virginia.
- Harrison, R., Watkins, P. T., Kier, R. J. (2007). "A low-power integrated circuit for a wireless 100-electrode neural recording system." *IEEE Journal of Solid-state Circuits*, 42, 123-133.
- Hitscherich, P., S. Wu, R. Gordan, L.-H. Xie, T. Arinzeh and E. J. Lee (2016). "The effect of PVDF-TrFE scaffolds on stem cell derived cardiovascular cells." *Biotechnology and Bioengineering*: n/a-n/a.
- Kasap, S. O. (2002). "Principles of Electronic Materials and Devices." New York: McGraw-Hill Companies.

- Lannutti, J., D. Reneker, T. Ma, D. Tomasko and D. Farson (2007). "Electrospinning for tissue engineering scaffolds." *Materials Science and Engineering: C* 27(3): 504-509.
- Leach, M. K., Z.-Q. Feng, S. J. Tuck and J. M. Corey (2011). "Electrospinning Fundamentals: Optimizing Solution and Apparatus Parameters." *Journal of Visualized Experiments : JoVE*(47): 2494.
- Peterson, K. E. (1998). "Silicon as a Mechanical Materials." *Proceeding of the IEEE*.
- Qing-Ming, W., D. Xiao-Hong, X. Baomin and L. E. Cross (1999). "Electromechanical coupling and output efficiency of piezoelectric bending actuators." *IEEE Transactions on Ultrasonics, Ferroelectrics, and Frequency Control* 46(3): 638-646.
- Sahay, R., V. Thavasi and S. Ramakrishna (2011). "Design Modifications in Electrospinning Setup for Advanced Applications." *Journal of Nanomaterials*.
- Sakaguchi, H., N. J. Amoroso and W. R. Wagner (2014). "Engineering Electrospun Scaffolds to Encourage Cell Infiltration." *springer book*.
- Salimi, A. and A. A. Yousefi (2003). "Analysis Method: FTIR studies of β -phase crystal formation in stretched PVDF films." *Polymer Testing* 22(6): 699-704.
- San Emerito, J. L. (1997). "Determination of electromechanical coupling factors of low Q piezoelectric resonators operating in stiffened modes. ." *IEEE Trans Ultrason Ferroelectr Freq Control*. Springer, New York, NY.
- Schwartz, R. E., J. Ballato, and G.H. Haertling. (2003). "Piezoelectric and Electrooptic Ceramics." *University of Missouri-Rolla*.
- Sharapov, V., Sotula, Zhanna, Kunickaya, Larisa (2014). "Piezo-Electric Electro-Acoustic Transducers." *Springer*
- Sharma, T., S. Naik, J. Langevine, B. Gill and J. X. J. Zhang (2015). "Aligned PVDF-TrFE Nanofibers With High-Density PVDF Nanofibers and PVDF Core–Shell Structures for Endovascular Pressure Sensing." *IEEE Transactions on Biomedical Engineering* 62(1): 188-195.
- Shirinov, A. V. and W. K. Schomburg (2008). "Pressure sensor from a PVDF film." *Sensors and Actuators A: Physical* 142(1): 48-55.
- Stroyan, J. J. (2004). "Processing and Characterization of PVDF, PVDF-TrFE and PVDF-TrFE-PZT Composites." *Master Thesis*.
- Tort, S. (2012). "Electrospinning."
- Vijaya, M. S. (2013). "Piezoelectric materials and devices." *CRC Press: Boca Raton, FL*.
- Zhang, D., Wang, D., Yuan, J., Zhao, Q., Wang, Z. , Cao, M. (2008). "Structural and electrical properties of PZT/PVDF piezoelectric nanocomposites prepared by cold-press and hotpress routes." *Chin. Phys. Lett*, 25.
- Zhu, G., Z. Zeng, L. Zhang and X. Yan (2008). "Piezoelectricity in β -phase PVDF crystals: A molecular simulation study." *Computational Materials Science* 44(2): 224-229.